

Contents

Introduction	3
1 Physical and Mathematical models	4
1.1 The concept of continuous medium and the notion of fluid particle	4
1.2 Description of the velocity field	4
1.2.1 Lagrangian or Eulerian description	4
1.2.2 Pathline vs Streamline	4
1.3 Main features of a fluid	5
1.3.1 Other fluid properties	6
1.4 Conservation laws	7
1.4.1 Particular or total derivative	8
1.4.2 Mass conservation law	8
1.4.3 Momentum conservation law	8
1.4.4 Energy conservation	10
1.5 Shock wave	12
2 ANSYS - FLUENT for compressible and incompressible fluids	12
2.1 Computational fluid dynamics (CFD)	12
2.2 Fluid Flow and Heat Transfer in a Mixing Elbow	13
2.2.1 Problem Description	13
2.2.2 Equations	14
2.2.3 Numerical results	14
2.3 Modeling Periodic Flow and Heat Transfer	17
2.3.1 Problem Description	17
2.3.2 Equations	17
2.3.3 Numerical results	18
2.4 Modeling Transient Compressible Flow : Nozzle simulation	19
2.4.1 Problem Description	19
2.4.2 Equations	19
2.4.3 Numerical results	20
2.5 Modeling External Compressible Flow : NACA 0012 simulation	23
2.5.1 Problem Description	23
2.5.2 Equations	23
2.5.3 Numerical results and analysis	23

3 elsA - ONERA software for compressible flows.	28
3.1 Naca test case	28
3.1.1 Problem Description	28
3.1.2 Equations	28
3.1.3 Numerical results	29
3.2 Shock tube test case	30
3.2.1 Problem Description	30
3.2.2 Equations	30
3.2.3 Numerical results	31
3.3 Nozzle test case	33
3.3.1 Problem Description	33
3.3.2 Equations	33
3.3.3 Numerical results	33

Introduction

Nowadays, the understanding of natural phenomena coming from Physics is taking an increasingly important place in companies through the Numerical Simulation of these ones. In fact, Numerical Simulation is a great tool that helps in the prediction, design and realization in many sectors of activity such as aeronautics, space, automotive, medical... The aim of the lecture was to address Numerical Simulation from the physical problem studied until its simulation using the dedicated software such as ANSYS-FLUENT and elsA-ONERA, thus it enabled us to link physical and mathematical modelling.

This report is dealing with the main models used in Newton fluid mechanics, probably the largest field of physics study due to its many applications. We will first present some generalities about fluid mechanics, going through the main features of the fluids, the conservation laws and the main mathematical equations governing physical phenomena. Then, we will present the various test cases carried out on the two software which enable to highlight the numerical steps to provide a good simulation and also which kind of simplifications and assumptions we must do in order to combine good approximation of the physical phenomena and a low computational cost.

1 Physical and Mathematical models

Fluid mechanics concerns the study of the motion of fluids, in general liquids and gases, in a flow and the strengths acting on them. As we consider mathematical model of the physical world, we need to make some basic assumptions about the medium studied. In this sense, laws of fluid mechanics are turned into equations which we are going to explain in this part.

1.1 The concept of continuous medium and the notion of fluid particle

As a part of continuum mechanics, fluid mechanics describe the flow at macroscopic scales, which assumes that a fluid can be regarded as a continuous medium. It means that we deal with the mechanical behavior as a continuous mass viewpoint rather than a discrete model based on atoms : it is a scheme that has the advantage of allowing the differential and integral calculation.

In such a way, a **fluid particle** is defined as a small volume element of the fluid large enough to contain various molecules : its size is small compared with the volume of all the body but large compared with the distance between molecules. In the sequel, when we will talk about the displacement of a fluid particle, it will be understood as the displacement of a volume element containing many atoms. The velocity vector of this particle will be taken as the average of the molecules' velocities which are part of it.

1.2 Description of the velocity field

1.2.1 Lagrangian or Eulerian description

There are two approaches to describe the velocity field of a fluid : the Lagrangian description and the Eulerian one.

In the first case, we consider that at the initial time t_0 the fluid is split into elementary fluid particles which are located on current point M_0 and we follow the movement of these particles along time. At a time t , we can define the velocity vector $\vec{v}(M_0, t)$ of the particle which was in M_0 at time t_0 . We define the trajectory of a fluid particle as the successive positions of this particle along time. From this point of view, an observer is linked to each fluid particle.

In the Eulerian description, we describe the fluid movement in fixed place, it means that we study the velocity of the fluid particle which is located in M , fixed, at time t : it is therefore a different particle at each time. This description is especially relevant in the case of steady flow which means that all the physical quantities do not vary locally along time. We will see later how we can characterize steady flows from a differential point of view.

1.2.2 Pathline vs Streamline

In order to describe a flow, we can represent the velocity field which corresponds to the path of the velocity vector $\vec{v}(M, t)$ at any point M and a given time t . Another approach commonly used is the **streamline** representation which must not be confused with the pathline. In the Lagrangian description, we obtain directly the trajectories or **pathline** of the fluid particle as defined in the previous section. However, the streamlines are the curves tangent to the velocity vector at a given instant.

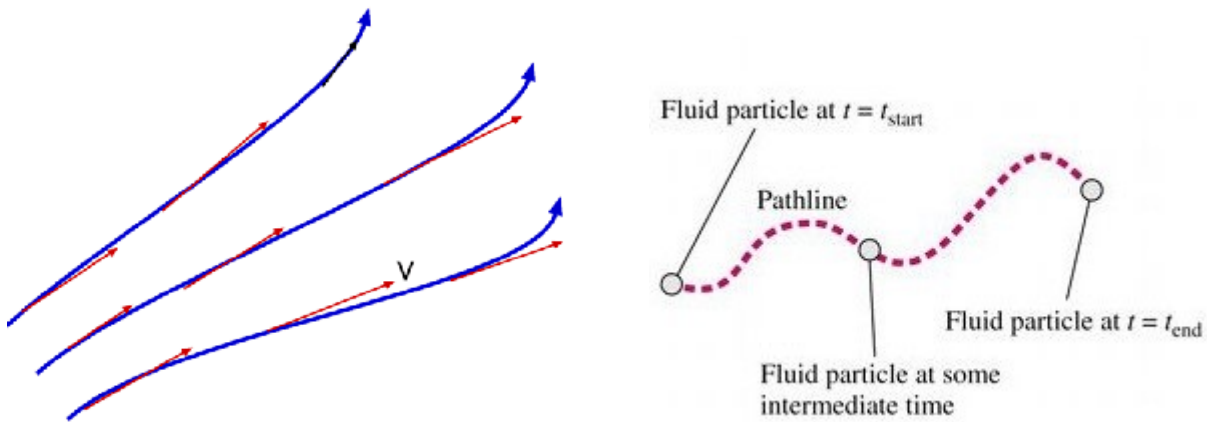


Figure 1: On the left : velocity field (in red) and streamlines (in blue). On the right : pathline.

1.3 Main features of a fluid

In order to characterize a fluid, we define some properties which are the principal unknowns when we consider flow equation : among them, the **velocity** \vec{v} , defined as the first derivative of the position vector, the **temperature** T , the **pressure** P and the **density** ρ , which is simply the amount of matter per unit of volume. There are, at the end, six primary unknowns (three scalars and one vector) and all the other properties of the fluid can be express as linear combination of these main features. As explained above, we will describe the fluid motion thanks to fluid particles which will be equipped with their own properties :

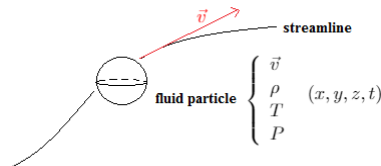


Figure 2: Fluid particle with its own properties in 4 dimensions.

Concerning the units of such properties, we use the classical one coming from the International System (SI) listed in the following table :

Physical quantity	Symbol, Dimension	Unit
length	[l]=L	meters (m)
time	[time]=T	seconds (s)
temperature	[temp]=K	kelvin (K)
mass	[mass]=M	kilogram (kg)
intensity	[int]=A	ampere (A)

With all this in mind, we can define the unit of the density as $[\rho] = ML^{-3} = kg.m^{-3}$ (mass M over a volume L^3). Since the pressure is defined as the norm of a strength out of the area on which we apply the strength, its unit is given by $[P] = \frac{[F]}{[S]}$ with $[F]$ the strength unit (in Newton) and $[S] = L^2$, the area unit. Knowing that $[F] = MLT^{-2}$, we have $[P] = ML^{-1}T^{-2} = kg.m^{-1}.s^{-2}$ which is commonly called Pascal (Pa). Finally, the unit of the velocity is $[\vec{v}] = LT^{-1} = m.s^{-1}$.

1.3.1 Other fluid properties

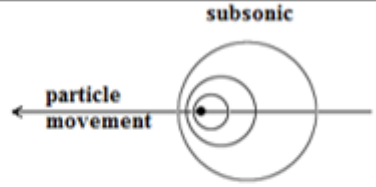
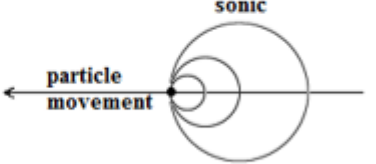
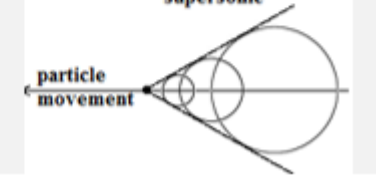
There are several other properties that enable to characterize a fluid flow, we are going to describe them in this part.

First, we can make some assumptions concerning the fluid like for instance **perfect gas** hypothesis that gives the following equation $Pv = nrT$ with P the pressure, v a volume, n the number of mole, $r = 8.314 \text{ J.mol}^{-1}.\text{K}^{-1}$ the perfect gas constant, T the temperature. Another way of written it is

$$P = \rho RT$$

where R is linked with r by $R = \frac{r}{M}$ and $\hat{M} = 29.9 \text{ gr.mol}^{-1}$ is the molar mass of air. At the end, for the air we have $\mathbf{R} = 287 \text{ J.kg}^{-1}.\text{K}^{-1}$.

At this point, we are able to define another important property which is whether the fluid is compressible or not. This is linked with density : if ρ is constant which means there is no variation in space and in time for the density, then the fluid will be **incompressible**. Otherwise, it will be **compressible**. We can relate the compressible character of a flow using the speed of sound thanks to the **Mach Number** which is defined as the ratio of the flow speed to the speed of sound. We must notice that for perfect gas and in atmospheric conditions¹, the speed of sound is expressed as $C = \sqrt{\gamma RT}$ with $\gamma = 1.4$, $T = 293.15\text{K}$, and $R = 287 \text{ J.kg}^{-1}.\text{K}^{-1}$ thus $C = 340\text{m.s}^{-1}$. We have the following repartition of flow regimes du to Mach number :

Mach Number	Flow regime	Representation
$M < 1$	Subsonic flow: the particle has a lower velocity than the increase of the spheres, due to the pressure perturbation, it creates at each moment.	
$M = 1$	Sonic flow	
$M > 1$	Supersonic flow: the particle leaves all the perturbation spheres behind. Shock wave	

Moreover, if $M < 0.3$ we consider that the fluid is incompressible. Finally, another way to say that a fluid is incompressible or not is to look at its divergence : in fact, if $\rho = cste$ it implies that

$$\vec{\nabla}(\rho \vec{v}) = 0 \Rightarrow \vec{\nabla} \cdot \vec{v} = \text{div } \vec{v} = 0.$$

There is no acoustic propagation (for example if the fluid is incompressible, we can't hear the talk because, there is no variation or propagation).

¹ $T_0 = 293,15 \text{ K}$, $P_0 = 101325 \text{ Pa}$ and $\rho_0 = 1,2 \text{ kg.m}^{-3}$

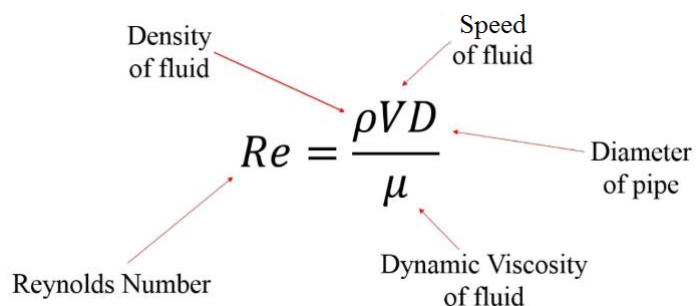
Among the other characteristics that defines a fluid, there are the dynamic viscosity μ (how fluid has friction capability) in Pa.s, the kinetic viscosity $\nu = \frac{\mu}{\rho}$, the thermal diffusion λ describing how easily the fluid transports energy (how easily heat insulted, example : λ is low in wood and high in iron) and C_p (heat capacity, amount of energy we need to heat 1 Kg for 1 Kelvin, ex : C_p in water is 4.19, in oil is 1.97 Kg/K, this means that to heat water of 1Kg/k we need double more energy), C_v the calorific capacity at constant pressure and volume respectively which are defined by :

$$C_v = \frac{R}{\gamma - 1} \quad \text{and} \quad C_p = \frac{\gamma R}{\gamma - 1}$$

with the previous definition of $\gamma = 1.4$ and $R = 287 \text{ J.kg}^{-1}.K^{-1}$.

Besides, we define a **perfect fluid** when it is possible to describe its movement without taking into account the effects of viscosity and thermal conduction λ : it means that these fluids have strictly zero viscosity, $\nu = 0$, hence they do not dissipate. Obviously, this is an idealization, which describes accurately flows far away from boundaries. In fact, this approximation means that we neglect friction effects, however it breaks down near boundaries because dissipation and friction effects concentrate in thin regions called "boundary layers".

Another characteristic quantity which describes the fluid flow is the **Reynold Number** : it is a dimensionless quantity defined by

$$Re = \frac{\rho V D}{\mu}$$


It represents the ratio of inertial forces given by the momentum to viscous forces and it describes how viscous is a fluid : the fluid can be either **laminar**, with less energy transfer, or **turbulent**. For external flow, for instance, we consider the flow as laminar if $Re < 10^5$ and turbulent if $Re > 10^5$.

1.4 Conservation laws

In physics, a conservation laws states that a particular property of an isolated physical system is conserve which means that it does not change as the system evolves over time. There are four main conservation laws in fluid mechanics : mass conservation, energy conservation, momentum conservation and finally an equation of state which concerns the features of the fluid.

The last equation is an assumption concerning the fluid : for instance, we can have perfect gas hypothesis as explained in the previous part.

1.4.1 Particular or total derivative

We denote $\chi \in \begin{cases} \vec{v} \\ \rho \\ P \\ T \end{cases}$ (x, y, z, t) and we want to express the total or particular variation, in the sense of fluid particle, by the following equation

$$\frac{d\chi}{dt}(x, y, z, t) = \frac{\partial\chi}{\partial x} \frac{dx}{dt} + \frac{\partial\chi}{\partial y} \frac{dy}{dt} + \frac{\partial\chi}{\partial z} \frac{dz}{dt} + \frac{\partial\chi}{\partial t}.$$

By pointing out that $\vec{v} = \frac{dx}{dt} \vec{x} + \frac{dy}{dt} \vec{y} + \frac{dz}{dt} \vec{z}$, we can rewrite the total variation over time $\frac{d\chi}{dt}$ as the sum of the local derivative $\frac{\partial\chi}{\partial t}$, which is a non stationary term, and a convective or Lagrangian term $(\vec{v} \cdot \vec{\nabla})\chi$:

$$\boxed{\frac{d\chi}{dt} = \frac{\partial\chi}{\partial t} + (\vec{v} \cdot \vec{\nabla})\chi} \quad (1)$$

We have already seen that for a **permanent or stationary fluid**, all the physical quantities do not vary locally along time thus using the equation (1), it means that the local derivative of the four parameters is equal to zero : $\frac{\partial\chi}{\partial t} = 0$.

1.4.2 Mass conservation law

In the sequel, we are going into the details of the conservation laws, starting with the mass conservation. We are dealing with a fluid particle with a given volume $\mathcal{V}_m(t)$ and the surface $\mathcal{A}_m(t)$ containing the volume. Mass is conserved means that the mass derivative with respect to time is equal to zero :

$$\frac{dm}{dt} = \frac{d}{dt} \int_{\mathcal{V}_m(t)} \rho \, dv = 0$$

then, we rewrite the total derivative as explained in equation (1) so we get

$$\int_{\mathcal{V}_m(t)} \left(\frac{\partial\rho}{\partial t} + \vec{\nabla} \cdot (\rho \vec{v}) \right) \, dv = 0.$$

Finally, it leads to the following mass conservation equation

$$\boxed{\frac{\partial\rho}{\partial t} + \vec{\nabla} \cdot (\rho \vec{v}) = 0}$$

1.4.3 Momentum conservation law

A momentum is a product of mass by velocity, which means that for fluid a momentum is given by $\rho \vec{v}$ with the usual notations. We must notice that the equivalent of the momentum conservation law for solid is the Fundamental Principle of Mechanics from Newton ($\sum \vec{F}_{ext} = m \vec{a} = \frac{d\vec{P}}{dt}$ with $\vec{P} = m \vec{v}$ a momentum). For a fluid, we related the sum of the external strength with an integral over a volume of the momentum :

$$\sum \vec{F}_{ext} = \frac{d}{dt} \int_{\mathcal{V}_m(t)} \rho \vec{v} \, dv \quad (2)$$

External strengths include the weight (coming from the gravity field)

$$\int_{\mathcal{V}_m(t)} \rho \vec{g} \, dv$$

and contact strength which is given by

$$\int_{\mathcal{A}_m(t)} T : \vec{n} = \int_{\mathcal{A}_m(t)} t(n) \, ds,$$

denoting T the symmetric stress tensor, the outward normal unit \vec{n} and $T : \vec{n}$ the product matrix vector. As we consider vectors, we have to project over the i^{th} direction thus the vector equation (2) becomes :

$$\int_{\mathcal{V}_m(t)} \rho g_i \, dv + \int_{\mathcal{A}_m(t)} t_i(n) \, ds = \frac{d}{dt} \int_{\mathcal{V}_m(t)} \rho v_i \, dv \quad (3)$$

with $t_i(n) = T_{i,j} \cdot n_j$ and using the Einstein notation for the summation of repeated indexes. Moreover, contact strength expressed by the stress tensor can be decomposed into dynamic stress coming from friction and static stress coming from pressure as follows

$$\boxed{\mathbf{T}_{i,j} = -P\delta_{i,j} + \tau_{i,j}}$$

with P the static pressure, $\delta_{i,j}$ the Kronecker symbol and $\tau_{i,j}$ the dynamic stress. It means that finally $t_i(n) = (-P\delta_{i,j} + \tau_{i,j})n_j$ thus with the Einstein notation we get :

$$\begin{aligned} t_1(n) &= -Pn_1 + \tau_{1,1}n_1 + \tau_{1,2}n_2 + \tau_{1,3}n_3 \\ t_2(n) &= -Pn_2 + \tau_{2,1}n_1 + \tau_{2,2}n_2 + \tau_{2,3}n_3 \\ t_3(n) &= -Pn_3 + \tau_{3,1}n_1 + \tau_{3,2}n_2 + \tau_{3,3}n_3. \end{aligned}$$

With such definition of the stress tensor, we can rewrite the contact strength

$$\int_{\mathcal{A}_m(t)} t_i(n) \, ds = \int_{\mathcal{A}_m(t)} (-P\delta_{i,j} + \tau_{i,j})n_j \, ds,$$

using the Ostrogradski formula we have

$$\int_{\mathcal{V}_m(t)} \frac{\partial}{\partial x_j} (-P\delta_{i,j} + \tau_{i,j}) \, dv = \int_{\mathcal{V}_m(t)} -\frac{\partial P}{\partial x_j} \, dv + \int_{\mathcal{V}_m(t)} \frac{\partial \tau_{i,j}}{\partial x_j} \, dv.$$

From equation (3), we get

$$\begin{aligned} \frac{d}{dt} \int_{\mathcal{V}_m(t)} \rho v_i \, dv &= \int_{\mathcal{V}_m(t)} \rho \frac{dv_i}{dt} \, dv = \int_{\mathcal{V}_m(t)} \left[\rho g_i - \frac{\partial P}{\partial x_i} + \frac{\partial \tau_{i,j}}{\partial x_j} \right] \, dv \\ \Rightarrow \rho \frac{dv_i}{dt} &= \rho g_i - \frac{\partial P}{\partial x_i} + \frac{\partial \tau_{i,j}}{\partial x_j}, \quad \forall i, \end{aligned}$$

which leads to the following **Navier-Stokes equation**

$$\boxed{\rho \frac{d\vec{v}}{dt} = \rho \vec{g} - \vec{\nabla} P + \vec{\nabla} \tau} \quad (4)$$

There is another way to write the Navier-Stokes equation using the equation (1) which decompose the total derivative into a stationary and a Lagrangian term, we obtain **Momentum Law**:

$$\boxed{\frac{d(\rho \vec{v})}{dt} = \frac{\partial}{\partial t}(\rho \vec{v}) + \vec{\nabla} \cdot (\rho \vec{v} \vec{v}) = -\vec{\nabla} P + \rho \vec{g} + \vec{\nabla} \tau}$$

We must notice that in the case of permanent fluid, where $\frac{\partial \vec{v}}{\partial t} = 0$, it remains from the particular derivative only the Lagrangian term, thus we have the modified expression of the Navier-Stokes equation

$$\rho(\vec{v} \cdot \vec{\nabla})\vec{v} = \rho\vec{g} - \vec{\nabla}P + \vec{\nabla}\tau.$$

We can also demonstrate that in the case of Newtonian fluids we have the following expression of the dynamic stress (due to friction) :

$$\tau_{i,j} = \mu \left(\frac{\partial v_i}{\partial x_j} + \frac{\partial v_j}{\partial x_i} \right) - \frac{2}{3}\mu \left(\frac{\partial v_k}{\partial x_k} \delta_{i,j} \right)$$

then we can compute the projection of the derivative $\vec{\nabla}\tau$:

$$\frac{\partial \tau_{i,j}}{\partial x_j} = \mu \vec{\nabla}^2 v_i + \frac{1}{3}\mu \frac{\partial}{\partial x_i} (\vec{\nabla} \cdot \vec{v}).$$

It means that if we consider an incompressible flow ($\vec{\nabla} \cdot \vec{v} = 0$), we have the following written of the Navier-Stokes equation, dividing by ρ each terms:

$$\frac{\partial \vec{v}}{\partial t} + \vec{\nabla} \cdot (\vec{v} \vec{v}) = -\frac{1}{\rho} \vec{\nabla}P + \nu \Delta \vec{v} + \vec{g} \quad (5)$$

Finally, in we consider the Navier-Stokes equation for perfect fluid we obtain what is called the **Euler equation**. It is equivalent to neglect the friction or viscosity effects near the boundaries, as explained before, and it means that we do not observe the boundary layer which is the region where heat and mass transfers and consequently where lost of energy appear. For the Euler equation, we do not consider anymore the dynamic stress τ so the sum of the forces is reduced to the gravity strength and contact strength. The Euler equation can be written as

$$\frac{\partial(\rho \vec{v})}{\partial t} + \vec{\nabla} \cdot (\rho \vec{v} \vec{v}) = -\vec{\nabla}P + \rho \vec{g}.$$

1.4.4 Energy conservation

We are going to build energy conservation : the main principle is the first law of thermodynamics, which, when applied to a moving fluid element becomes : the total variation of energy over the time of a fluid particle is equal to the sum of heat exchanges and the work variation of each strengths.

The total energy of fluid particle is the sum of kinetic energy $\frac{\rho v^2}{2}$ and internal energy $U = \rho e$. The internal energy is linked with temperature and we use the usual notation $e = C_v T$.

First law of thermodynamic

$$\boxed{\frac{d}{dt} \int_{V_m(t)} \left(\frac{1}{2} \rho v^2 + \rho C_v T \right) dv = \dot{W} + \dot{Q}} \quad (6)$$

where $\dot{W} = \frac{d}{dt} W$ comes from the external strength (gravity) and contact strengths (static and friction).

As the work is defined by the product of a strength by a distance $W = F \times L$ and we know that $[F] = M L T^{-2} \rightarrow$ Newton, we have $[W] = M L T^{-2} \times L \rightarrow$ Joule. And finally

$$[\dot{W}] = \left[\frac{d}{dt} W \right] = \frac{M L^2 T^{-2}}{T} = M L^2 T^{-3} \rightarrow \text{Watt}.$$

Regarding to the units, we can observe that the work variation can be seen as the product of a strength by a speed v : $\dot{W} = F \times v$. We set

$$\dot{W} = \int_{V_m(t)} \rho \vec{g} \vec{v} dv + \int_{A_m(t)} t(n) \vec{v} dS.$$

Heat exchange between the isolated system and the outside is propagated by conduction: it means that we consider only conduction transfer and we suppose no internal production of energy inside. So, we can write the heat exchanges as :

$$\dot{Q} = \frac{d}{dt} Q = - \int_{A_m(t)} \vec{q} \cdot \vec{n} dS$$

where $\vec{q} = \lambda \vec{\nabla} T$ (we recall that λ is the thermal conductivity and \vec{q} is coming from Fourier's law.) With such definitions of the work variation and heat exchanges, equation (6) becomes :

$$\frac{d}{dt} \int_{V_m(t)} \rho (e + \frac{1}{2} v^2) dv = \int_{V_m(t)} \rho \vec{g} \vec{v} dv + \int_{A_m(t)} t(n) \vec{v} dS - \int_{A_m(t)} \vec{q} \cdot \vec{n} dS$$

where $t_i(n) = -P n_i + \tau_{ij} n_j$ (with the Einstein notation). Let us develop the right hand side terms using Ostrograski formula :

$$\begin{aligned} \int_{A_m(t)} t(n) \vec{v} dS &= \int_{A_m(t)} (-P n_i v_i + \tau_{ij} n_j) dS \\ &= \int_{V_m(t)} \left(\frac{\partial}{\partial x_i} (-P v_i) + \frac{\partial}{\partial x_j} (\tau_{ij} v_i) \right) dv \end{aligned}$$

and

$$\int_{A_m(t)} -\vec{q} \cdot \vec{n} dS = \int_{V_m(t)} -\frac{\partial}{\partial x_i} q_i dv.$$

But, using

$$\frac{d}{dt} \int_{V_m(t)} \rho \phi dv = \int_{V_m(t)} \rho \frac{d\phi}{dt} dv$$

we have

$$\rho \frac{d}{dt} (e + \frac{1}{2} v^2) = \underbrace{\rho \vec{g} \vec{v}}_{\text{gravity strength}} - \underbrace{\vec{\nabla}(P \vec{v}) + \vec{\nabla}(\tau \cdot \vec{v})}_{\text{surface strengths}} - \underbrace{\vec{\nabla} \vec{q}}_{\text{variation of heat transfer}}.$$

We also recall that

$$\frac{d}{dt} \int_{V_m(t)} \square dv = \int_{V_m(t)} \frac{\partial \square}{\partial t} dv + \vec{\nabla}(\square \cdot \vec{v}) dv$$

therefore the equation above can be written as :

$$\frac{\partial \rho (e + \frac{1}{2} v^2)}{\partial t} + \vec{\nabla} \rho (e + \frac{1}{2} v^2) \vec{v} = \rho \vec{g} \vec{v} - \vec{\nabla}(P \vec{v}) - \vec{\nabla}(\tau \cdot \vec{v}) - \vec{\nabla} \vec{q}$$

that is to say,

$$\frac{\partial \rho (e + \frac{1}{2} v^2)}{\partial t} + \vec{\nabla} \rho (e + \frac{1}{2} v^2 + \frac{P}{\rho}) \vec{v} = \rho \vec{g} \vec{v} + \vec{\nabla}(\tau \cdot \vec{v}) - \vec{\nabla} \vec{q}.$$

In conclusion and denoting by $E = e + \frac{1}{2} v^2$, we have the scalar **Energy Law** :

$$\frac{\partial \rho E}{\partial t} + \vec{\nabla} (\rho E \vec{v} + P \vec{v} - \tau \vec{v} + \vec{q}) = \rho \vec{g} \vec{v}$$

(7)

If we summarize, all the conservation laws for Newtonian fluids are given by :

Energy Law :

$$\frac{\partial \rho E}{\partial t} + \vec{\nabla} (\rho E \vec{v} - T(n) \vec{v} + \vec{q}) = \rho \vec{g} \vec{v}$$

Momentum Law or N.S.equation :

$$\frac{\partial \rho \vec{v}}{\partial t} + \vec{\nabla} (\rho \vec{v} \vec{v} + P \delta - \tau) = \rho \vec{g}$$

Mass equation Law :

$$\frac{\partial \rho}{\partial t} + \vec{\nabla} (\rho \vec{v}) = 0$$

where we will add an equation of state to have a closed system.

1.5 Shock wave

Shock wave occurs when the flow goes from high velocity (supersonic : $M > 1$) to a low velocity (subsonic : $M < 1$), we notice that the pressure and temperature increases but the velocity is decreases.

The plane does not damage during the shock waves, because the Wave come from contact of body with air, so wave goes out. The driver of the plane stay cool, since the shock wave is in front of him.

To know the place where the shock wave is and where there is variation in velocity through the stream line, we have to compute the **entropy** $S = \ln(\frac{P}{\rho^\gamma})$ which characterize the disorder of atoms and molecules. $S \geq 0$ and if $S = cst$ then there is no shock wave.

2 ANSYS - FLUENT for compressible and incompressible fluids

2.1 Computational fluid dynamics (CFD)

Creating numerical modeling for what we are studying, and apply law of physics and see how things flow.

ANSYS : Is a software doing fluid dynamics. CFD based on FVM, in each control volume (cell) we will solve the transport equation for : Mass, Momentum and energy.

- First step : Define the domain, reduce the complexity from 3D to 2D if it is possible and focus on the shape of profile.
- Second step : Define the mesh, mesh discretization, define general settings, general pressure base (correspond for numeric in incompressible low velocity $M < 0.3$) or density base (compressible $M > 0.3$).
- Third step : Define the fluid (air, water) and decide the physics to know equations that we want to solve. Steady, transient, laminar and turbulent.
- Fourth step : Boundary conditions, boundary layer (is the surface where the velocity increases until it reaches the infinite value).
- Fifth step : Solve, we have to define the numeric schemes.

- Sixth step : Post-process.

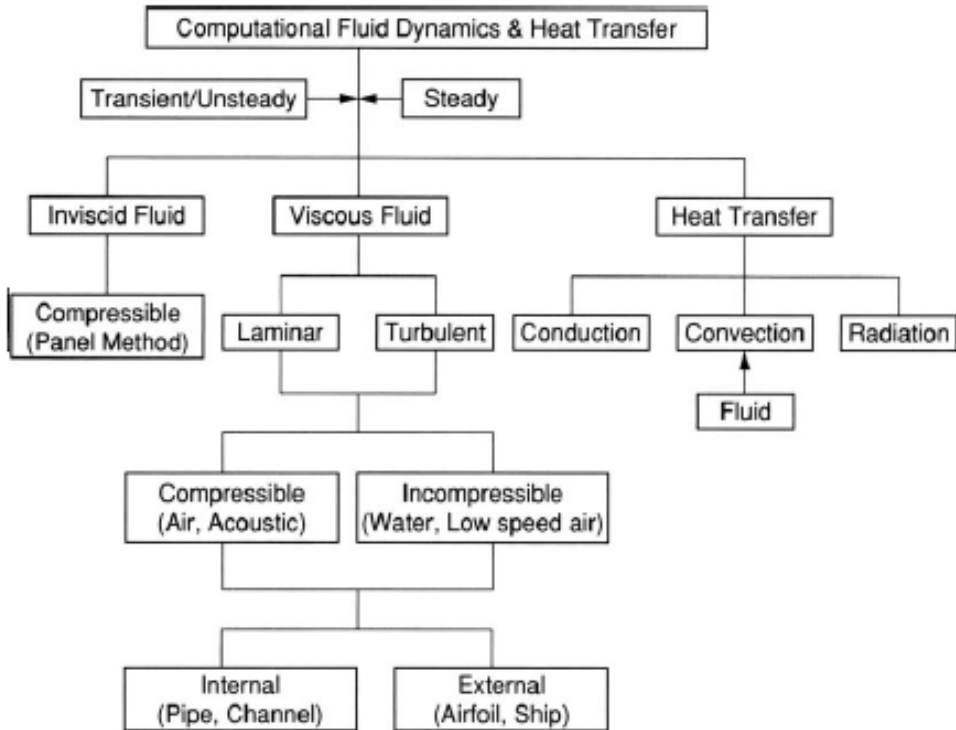


Figure 3: Tree decision for modelling choices.

2.2 Fluid Flow and Heat Transfer in a Mixing Elbow

2.2.1 Problem Description

This tutorial illustrates the setup and solution of a three-dimensional turbulent fluid flow and heat transfer problem in a mixing elbow. The mixing elbow configuration is encountered in piping systems in power plants and process industries. It is often important to predict the flow field and temperature field in the area of the mixing region in order to properly design the junction. The problem to be considered is shown schematically in Figure 4.

A cold fluid at 20°C flows into the pipe through a large inlet, and mixes with a warmer fluid at 40°C that enters through a smaller inlet located at the elbow. The pipe dimensions are in inches and the fluid properties and boundary conditions are given in SI units. The Reynolds number for the flow at the larger inlet is 50800 so a turbulent flow model will be required. As a matter of fact, for internal flow we consider a turbulent model for a Reynolds number $Re > 3000$.

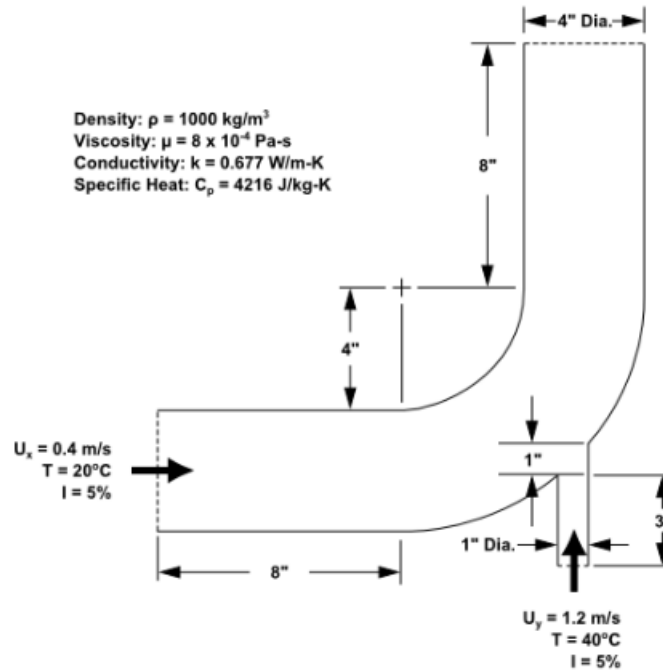


Figure 4: Elbow geometry and main properties. Since the geometry of the mixing elbow is symmetric, only half of the elbow must be modeled in ANSYS Fluent.

2.2.2 Equations

For this test case, we consider an **incompressible** flow with $\rho = \text{cste}$ since the fluid involved is liquid water with its usual properties : it means that we will use the pressure-based solver. We consider a **steady flow** thus $\frac{\partial \chi}{\partial t} = 0$, and we will use the k-epsilon **turbulent** model $Re = 50800$ (which add two equation to the numerics) with enhanced wall treatment since we want to capture the boundary layer due to wall friction. We will neglect gravity effects into the elbow. With all this in mind, it means that we will use the Navier-Stokes equation for incompressible flow as the momentum law and consequently the system of equations involved is :

$$\begin{cases} \operatorname{div} \vec{v} = 0 \\ (\vec{\nabla} \cdot \vec{v}) \vec{v} = -\frac{1}{\rho} \vec{\nabla} P + \nu \Delta \vec{v} \\ \vec{\nabla} (\rho E \vec{v} + P \vec{v} - \tau \vec{v} + \vec{q}) = 0 \end{cases}$$

Concerning the boundary conditions, we impose the values of the velocity vector and temperature on each inlets according to the Figure 4 with a turbulent intensity of 5%. At the outlet, we impose a zero heat flux.

2.2.3 Numerical results

We use both a residual convergence criterion and a number of iterations (150 iterations) to end the simulation. In this case, the solution is stopped when the convergence criterion on outlet temperature is satisfied, after approximately 75 iterations (see Figure 5). The exact number of iterations for convergence will vary, depending on the platform being used.

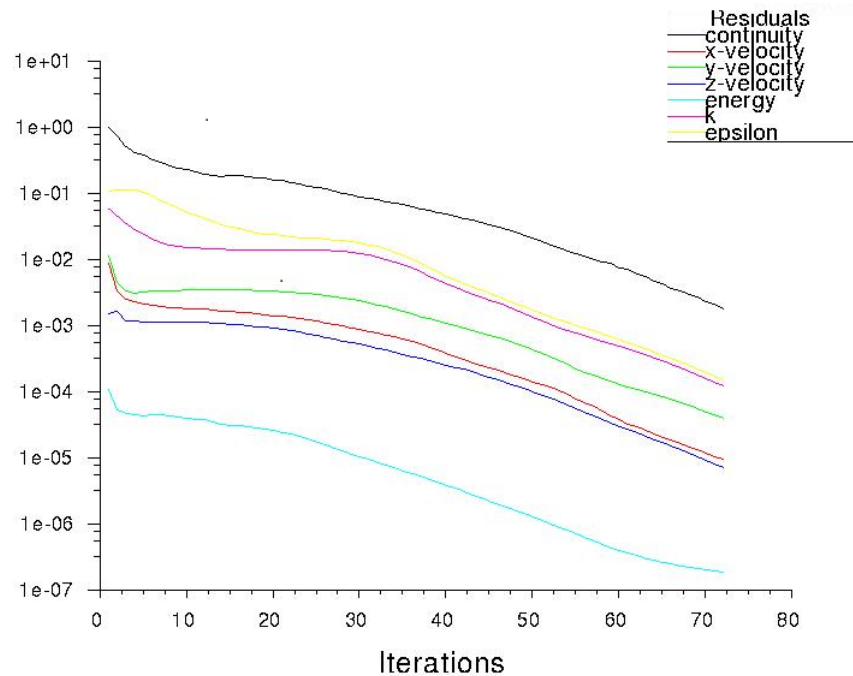


Figure 5: Residuals convergence curves.

After the simulation, we get the following results for the temperature and the velocity :

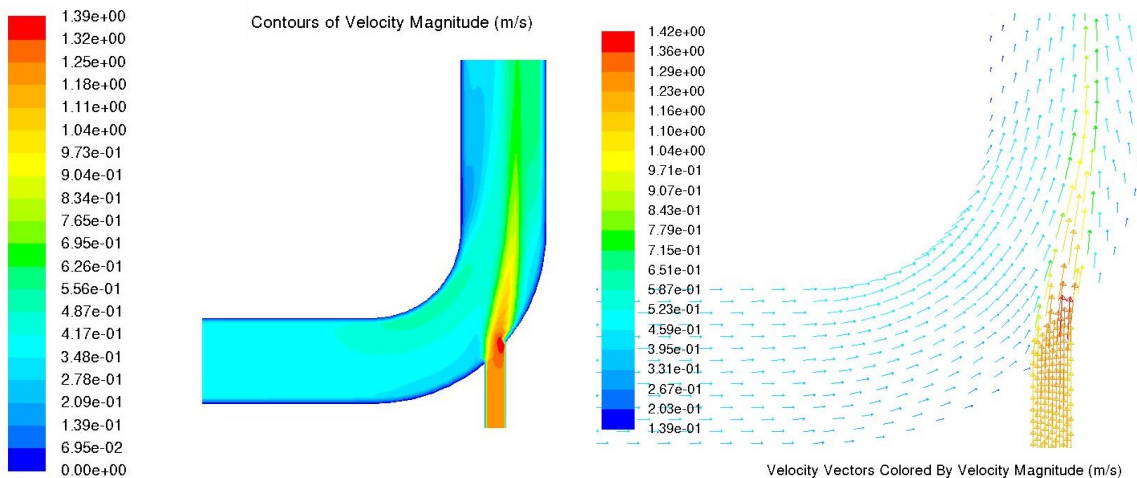


Figure 6: Velocity magnitude and velocity vectors.

The injection of the warmer fluid through the smaller inlet is done with a high velocity as we can see it on the Figure above. As we are in a turbulent model, we notice a reduction of the speed after the elbow precisely due to the characteristic shape of the pipe. When we are looking at the temperature field, we see that the warm fluid is increasing the temperature of the mixing after the elbow : the velocity and temperature contours are consistent.

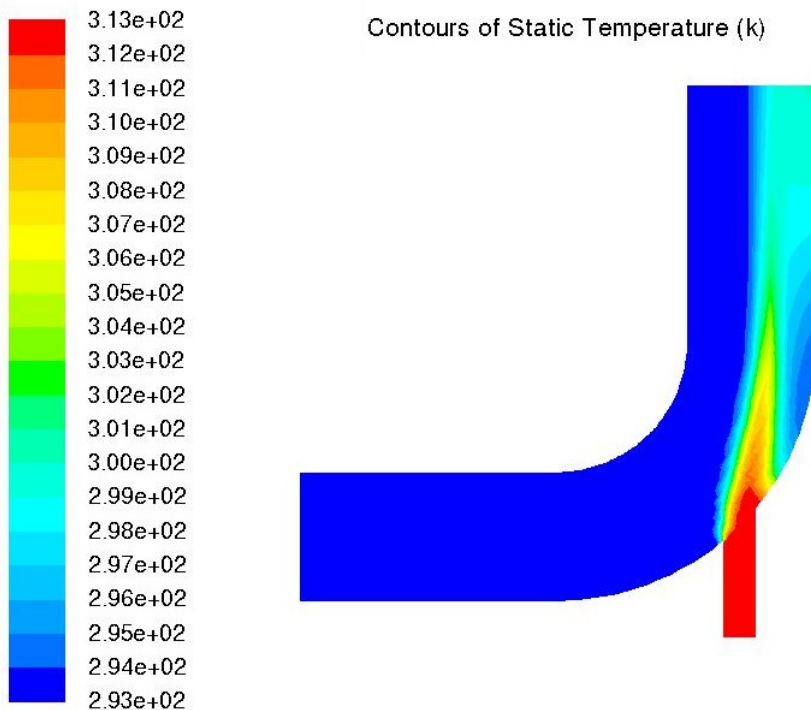


Figure 7: Temperature field in the elbow.

In order to improve the convergence speed, we can change the solver method : in fact the elbow solution computed in the first part used a simple solver scheme for pressure-velocity coupling. But for many general fluid flow problems the convergence speed can be improved by using the coupled solver. When we change the solver into coupled, we have convergence of the residuals after only 36 iterations.

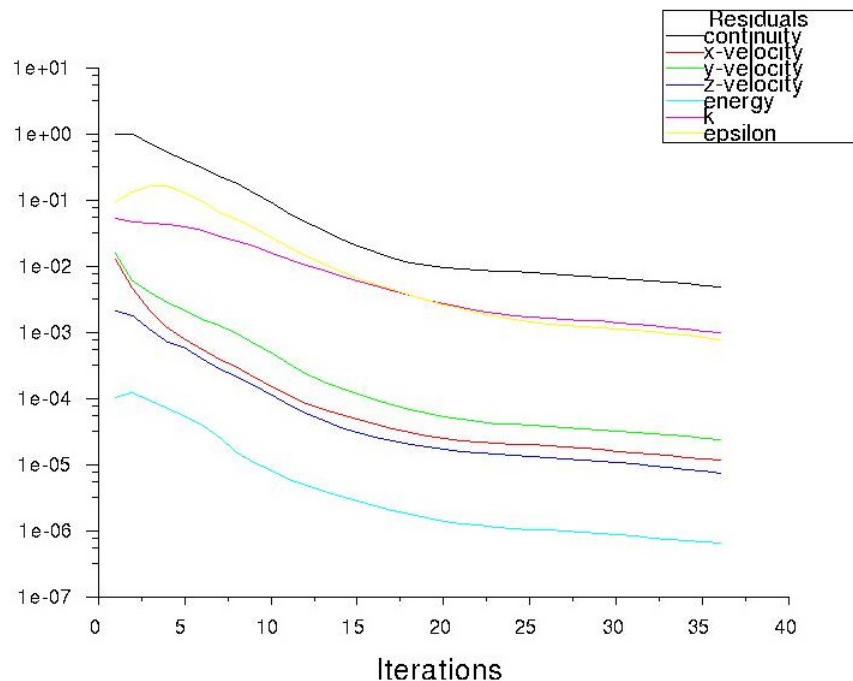


Figure 8: Residuals convergence curves for coupled scheme.

2.3 Modeling Periodic Flow and Heat Transfer

2.3.1 Problem Description

Many industrial applications, such as steam generation in a boiler or air cooling in the coil of an air conditioner, can be modeled as two-dimensional periodic heat flow. This tutorial illustrates how to set up and solve a periodic heat transfer problem, given a pre-generated mesh. The system that is modeled is a bank of tubes containing a flowing fluid at one temperature that is immersed in a second fluid in cross flow at a different temperature. The aim is to predict the flow and temperature fields that result from convective heat transfer.

This problem considers a 2D section of a tube bank as shown in Figure 9. The bank consists of uniformly-spaced tubes with a diameter of 1 cm, which are staggered across the cross-fluid flow. Their centers are separated by a distance of 2 cm in the direction, and 1 cm in the direction. The bank has a depth of 1 m.

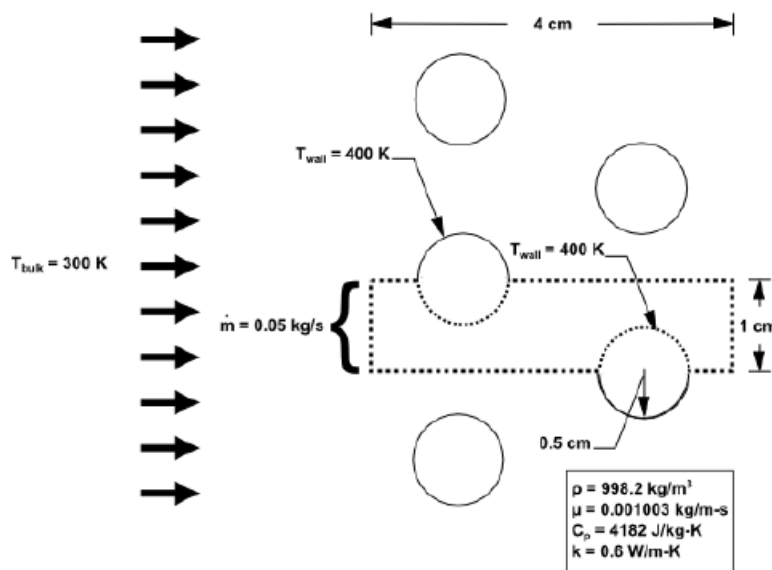


Figure 9: Problem Specification : due to symmetry of the tube bank only a portion of the geometry will be modeled in ANSYS Fluent. The real mesh considered is the area in dotted line.

2.3.2 Equations

Both fluids are water liquid, and the flow is classified as **laminar**, as we have a low Reynolds number of approximately 100, and **steady**. As we consider a laminar model, from the numerical point of view we will only consider the Navier-Stokes equation without any additional equation (as we have for turbulent models). The fluid is **incompressible** thus we use the pressure-based solver : it means that we will have a divergence condition as the mass conservation law, and the Navier-Stokes equation will be under the incompressible form. The main equations governing the convective heat transfer are :

$$\begin{cases} \operatorname{div} \vec{v} = 0 \\ (\vec{\nabla} \cdot \vec{v}) \vec{v} = -\frac{1}{\rho} \vec{\nabla} P + \nu \Delta \vec{v} \\ \vec{\nabla} (\rho E \vec{v} + P \vec{v} - \tau \vec{v} + \vec{q}) = 0 \end{cases}$$

where gravity is neglected. Concerning the boundary conditions, a mass flow rate of 0.05 kg/s is applied to the inlet boundary of the periodic module. The temperature of the tube wall (T_{wall}) is 400 K and the bulk temperature of the cross flow water (T_{bulk}) is 300 K.

2.3.3 Numerical results

As explained in the previous test case, we use here a coupled solver for pressure-velocity to improve the convergence speed of the numerics. We have convergence of the residuals after about 56 iterations and we get the following results :

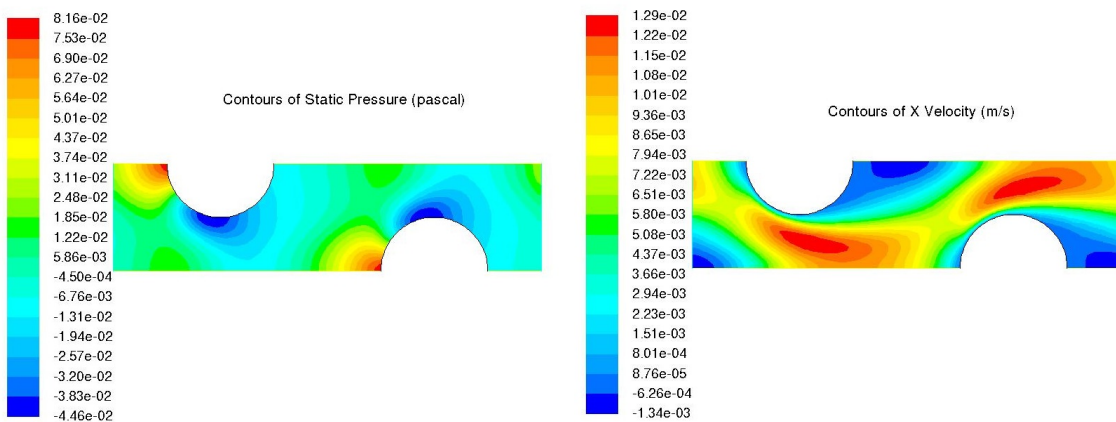


Figure 10: Representation of the static pressure and x-velocity fields.

We notice that the x-velocity is going around the tubes and we observe some recirculation of flow after the tubes since we have negative velocity in the deep blue areas. Concerning the pressure, we see high pressure zones just in front of the tubes and low pressure after them, which is consistent.

On the Figure 11, we have the evolution of temperature along the domain and we notice that the cold water, injected on the left, is becoming warmer after entering in contact with the warm tubes.

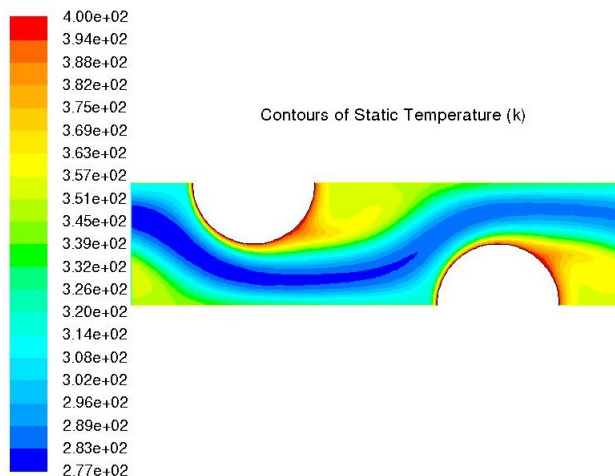


Figure 11: Temperature field.

2.4 Modeling Transient Compressible Flow : Nozzle simulation

2.4.1 Problem Description

In this tutorial, ANSYS Fluent's density-based implicit solver is used to predict the time-dependent flow through a two-dimensional nozzle. As an initial condition for the transient problem, a steady-state solution is generated to provide the initial values for the mass flow rate at the nozzle exit. The geometry to be considered in this tutorial is shown in Figure 12.

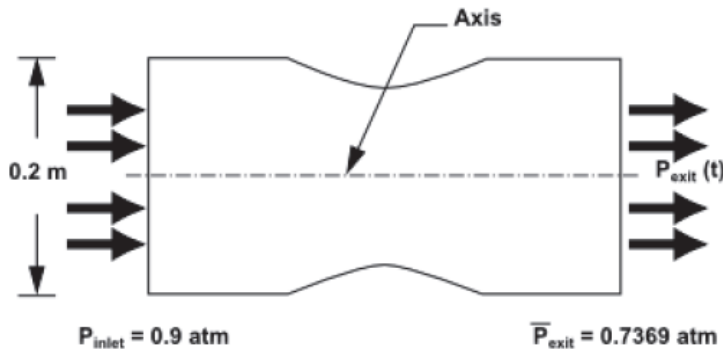


Figure 12: Problem Specification : whole 2-dimensional domain including symmetry axis. Due to symmetry, only half of the nozzle is modeled.

Flow through a simple nozzle is simulated as a 2D planar model. The nozzle has an inlet height of 0.2m, and the nozzle contours have a sinusoidal shape that produces a 20% reduction in flow area.

2.4.2 Equations

We denote by pressure upstream : $P_{up} = 0.9$ atm and pressure downstream : $P_{down} = 0.7369$ atm. The pressure variation between the two extremities of the nozzle gives the intensity of the velocity according to the following relation :

$$\frac{P_{up}}{P_{down}} = \left(1 + \frac{\gamma - 1}{2} M^2\right)^{\frac{\gamma}{\gamma - 1}} \quad (8)$$

Here we are work in ambient condition, that means the pressure is expressed in atmospheric unit, the temperature is 20°C and $\gamma = 1.4$. The equation above implies that $M = 0.54 > 0.3$ thus the fluid is compressible, that is why we used the density-based solver.

At the beginning, we thus consider a **compressible, subsonic steady flow** neglecting gravity effects. Besides, we deal with a **turbulent** model regarding to the air viscosity, and we take air as an **ideal gas** which means that the main equations on this problem are given by:

$$\begin{cases} \vec{\nabla} \cdot (\rho \vec{v}) = 0 \\ \vec{\nabla} \cdot (\rho \vec{v} \vec{v}) = -\vec{\nabla} P + \vec{\nabla} \tau \\ \vec{\nabla} \cdot (\rho E \vec{v} + P \vec{v} - \tau \vec{v} + \vec{q}) = 0 \\ P = \rho R T \end{cases}$$

where gravity is neglected. Concerning the boundary conditions, we first take no slip wall condition (we will see later that it provides a lower approximation of the Mach number than

what was expected) which enables to take into account friction phenomena, symmetry condition on the top boundary, and we impose static pressure values at the inlet and outlet boundaries (as given in Figure 12).

As a remark, when we will consider slip-wall boundary condition, it means that we will neglect friction effects, the fluid can be regarded as a perfect fluid thus we will consider the Euler equation instead of the Navier-Stokes one.

2.4.3 Numerical results

The problem is that we have computed using equation (8) an isentropic Mach number and we have $M_{Isentropic} = M_{Theoretical} = 0.54$ whereas $M_{CFD} = M_{Noslip} = M_{Friction} = 0.528$ after the simulation. Now, when we cancel the friction and compute the Mach number, we notice that $M_{Slip} = 0.5399$ which is closed to $M_{Isentropic} = 0.54$. In the sequel, we conserve the slip-wall condition since it provides a better approximation of the Mach number. It means that we have to change the boundary condition concerning the wall.

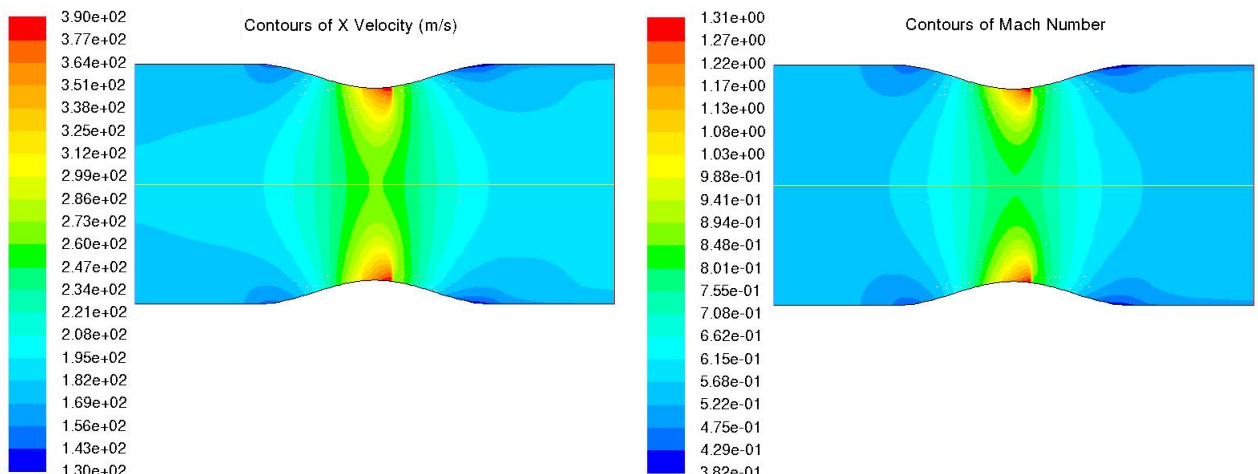


Figure 13: Mach number and x-velocity for a steady state and slip-wall condition.

Here we have subsonic case $M = 0.54 < 1$, the speed of sound is greater than the speed of flow, it means that the changes in pressure which occur downstream send pressure waves travelling upstream and impact the velocity. In the supersonic case, $M = 1.3 > 1$ for instance, outlet pressure has changed and can't go upstream. For a given inlet pressure $P_{up} = 0.9$, we can impose an outlet static pressure P_{down} such that we have either subsonic or supersonic cases. For examples, when $M = 1.3$, we calculate P_{down} and get it equal to 0.3248. When $M = 1.1$ we get $P_{down} = 0.42$ which is logical as Mac number decreased from 1.3 to 1.1 the outlet pressure increased from 0.32 to 0.42.

In a second time, we enable time-dependence by taking a transient time solver. It means that the local derivative is not equal to zero anymore thus the equations coming from conservation laws are now involving particular/total derivatives. We still consider subsonic flow in this case with $M = 0.54$ and slip-wall boundary condition. As we consider a transient flow, we can compute the Mach number at different times to see the evolution.

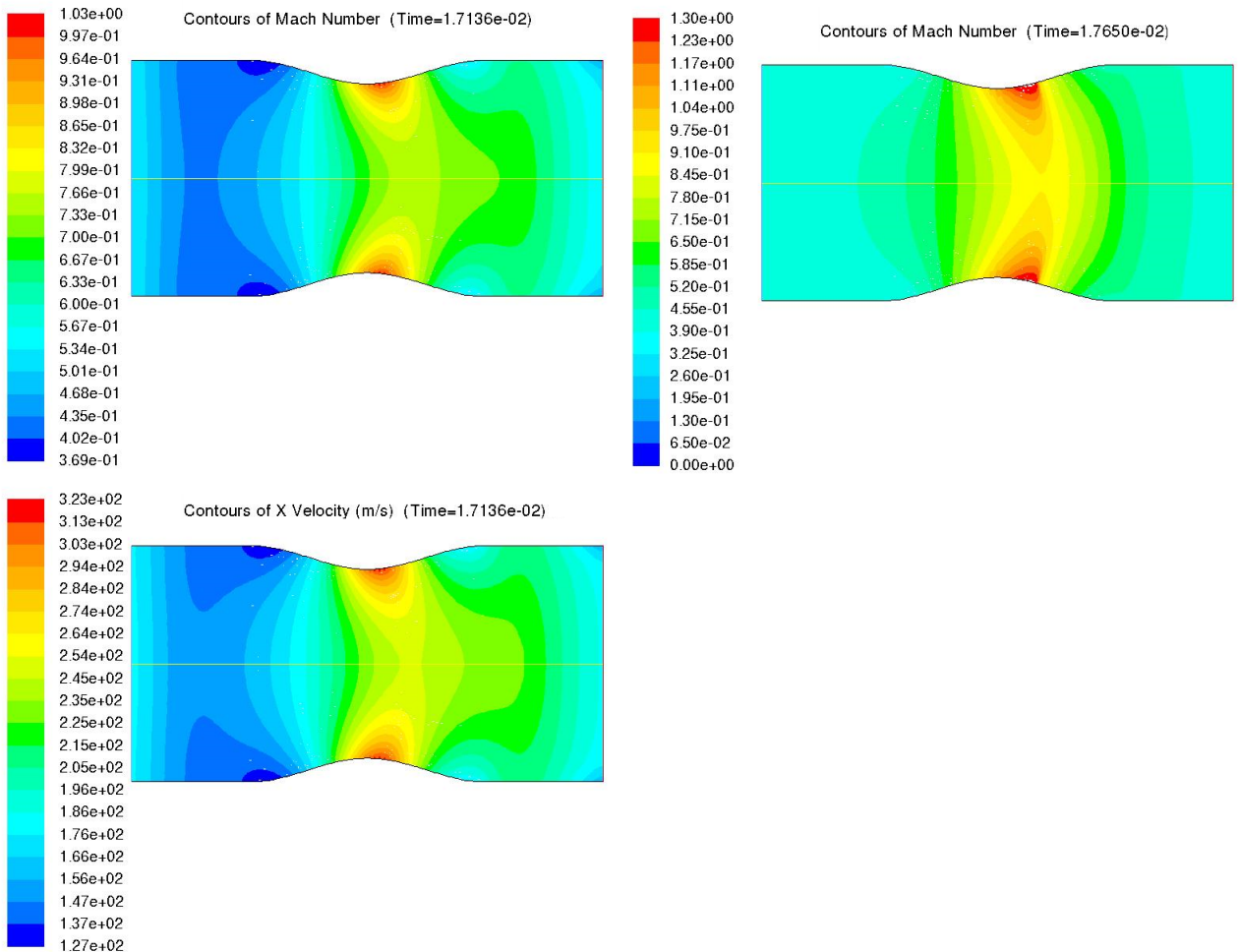


Figure 14: Evolution of the Mach number at two different times and x-velocity for transient flow.

Now, we want to observe a shock wave through the nozzle : we know that shock wave is happened when suddenly physical quantities change, there is an increase of all thermodynamical parameters (pressure, temperature, density increase whereas speed and mach decrease suddenly). In the sequel, we will take a supersonic case $M = 1.3$ by imposing $P_{down} = 0.3248$ as explained before (the information or the outlet pressure can't go upstream because the velocity of the flow is so high).

Let us create a line through the shock and recognize the static pressure : from the graph below we realise that the pressure starts from $0.74 \neq 0.9$ then accelerates and decreases until it reaches $0.25 \neq 0.3248$, where the Mac number is accelerated and increased until it reaches 1.6.

At some point there is discontinuity and flow compressed suddenly, to get the pressure back to 0.3248 : the shock happened and this before the pressure get back (that is why we have a lower pressure than expected).

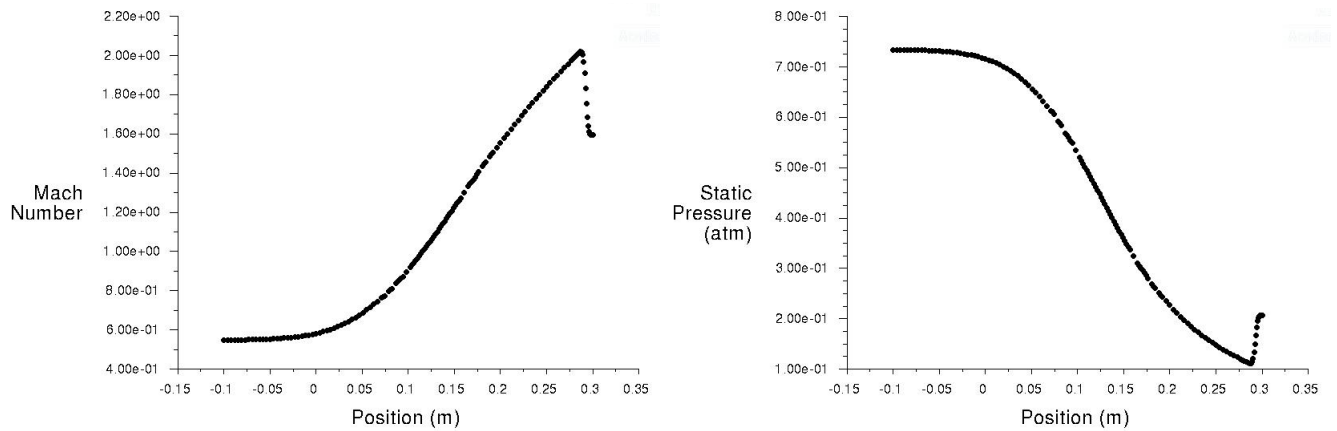


Figure 15: Spatial evolution of the static pressure and Mach number through the shock wave.

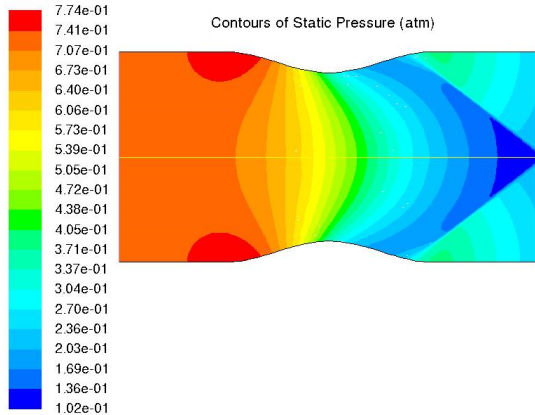


Figure 16: Static pressure : representation of the shock by pressure drop.

On the other hand, if we compare with subsonic case, when $M = 0.5$ we have $P_{down} = 0.758$ here we don't have shock and there is no discontinuity in the spatial variation of the physical quantities. The pressure start decreasing from 0.77 until it reaches 0.1 on the throat and then increases to 0.76 and the Mac number increases from 0.48 until it reaches the throat and then decreases again.

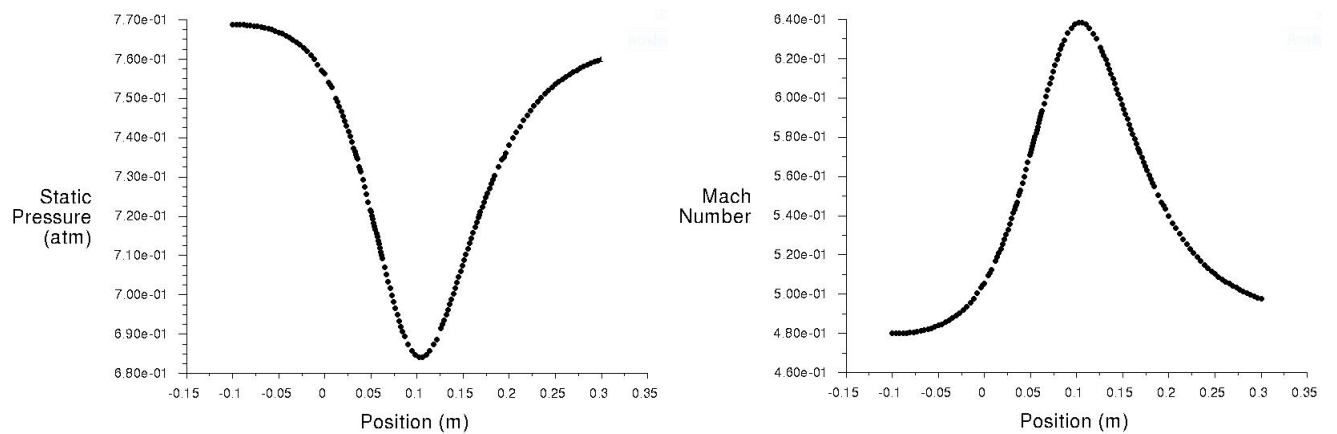


Figure 17: Spatial evolution of the Mach number in subsonic case.

2.5 Modeling External Compressible Flow : NACA 0012 simulation

2.5.1 Problem Description

The purpose of this tutorial is to compute the turbulent flow past a transonic airfoil at a nonzero angle of attack. The problem considers the flow around an airfoil at an angle of attack $\alpha = 4^\circ$ and a free stream Mach number of 0.5 ($M_\infty = 0.5$). The flow is transonic, and has a fairly strong shock near the mid-chord on the upper (suction) side. The chord length is 1m. The geometry of the airfoil is shown in Figure 18.

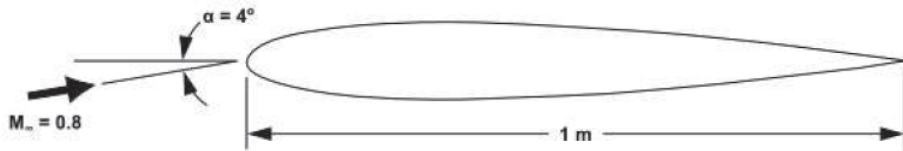


Figure 18: Problem Specification : 2D model with low geometric complexity.

2.5.2 Equations

We are going to deal with a **steady** and **turbulent Navier-Stokes** flow, we will first use the Spalart-Allmaras turbulence model (which add an equation to the usual conservation laws system to enable to accelerate the solution from a numerical point of view). Air is considered as an **ideal gas** (compressibility factor is 1) for the equation of state. Usually, the Mach number of an aircraft is around 0.8 thus we deal with **compressible flow**. However, we will use in Fluent the pressure-based solver with the coupled scheme (coupling pressure and velocity) since it is a good alternative to density-based solvers of ANSYS Fluent when dealing with applications involving high-speed aerodynamics with shocks. It means that the equation governing the flow are the following in the real case (neglecting gravity effects):

$$\begin{cases} \vec{\nabla} \cdot (\rho \vec{v}) = 0 \\ \vec{\nabla} \cdot (\rho \vec{v} \vec{v}) = -\vec{\nabla} P + \vec{\nabla} \tau \\ \vec{\nabla} (\rho E \vec{v} + P \vec{v} - \tau \vec{v} + \vec{q}) = 0 \\ P = \rho R T \end{cases}$$

while for the numeric scheme, it is imposed $\text{div} \vec{v} = 0$ since we use the pressure-based solver (for incompressible flow).

2.5.3 Numerical results and analysis

As we have friction, this means that we will loss energy in the profile. Moreover, we are going to study two variables : the angle of attack α and the Mach number M_α and also study their influence on lift and drag. For example, we are going to take different values of α between 0° and 14° , and at the same time $M_\alpha = 0.5$ or 0.7 .

When $\alpha = 0$ air arrives perfectly align with the profile, this means there is no lift and there is no suction or pressure side. At the contrary, when there is a non zero angle of attack, the velocity increases on the upper side of the wing (since the path is longer than on the lower

part of the wing) thus the pressure decreases creating a suction side. On the lower side of the wing, it creates a pressure side by an increase of pressure. This variation of pressure generate a strength from high pressure to low pressure area : it is the lift. We can also defined the drag as the strength coming from friction which is opposed to the movement. From an engineering point of view, we want to minimize the drag as it consumes aircraft fuel and optimize the lift. The paradox is that more velocity implies more friction and thus more drag, and a high velocity implies a higher pressure difference which implies higher lift.

We denote by C_L the lift coefficient and by C_d the drag coefficient. The lift coefficient is defined as the ratio of the lift strength by the energy of the flow (product of the dynamic pressure $q = 0.5\rho v^2$ by the surface S) and in the same wadefine the drag coefficient

$$C_L = \frac{F_L}{qS} \quad \text{and} \quad C_d = \frac{F_d}{qS}.$$

For $M_\alpha = 0.5$ and the Spalart-Allmaras turbulence model, we have the following table :

α	0	4	8	10	14
C_d	7.75887e-3	9.61833e-3	2.13x 10 ⁻²	1.461x 10 ⁻²	0.102712
C_L	0	0.5119	0.94539	0.913701	0.73045

Now for another turbulent model, k-epsilon, with same Mac number $M_{alpha} = 0.5$ we have the following table :

α	0	4	8	10	14
C_d	8.57E-03	9.90E-02	0.120899	0.1064	0.13497
C_L	0	4.99E-01	0.931517	0.853614	0.86361

The aim is to find the turbulent model which corresponds well to the experimental results. That is why we compute the drag and lift coefficient with respect to α and Mach number in order to compare them with the reference curves (given in the reference **1973 Gregory Wilby High Mach Number**).

Let us consider each case for $\alpha = 0^\circ, 4^\circ, 8^\circ$ and 14° and for same $M_\alpha = 0.5$

For $\alpha = 0$ we have :

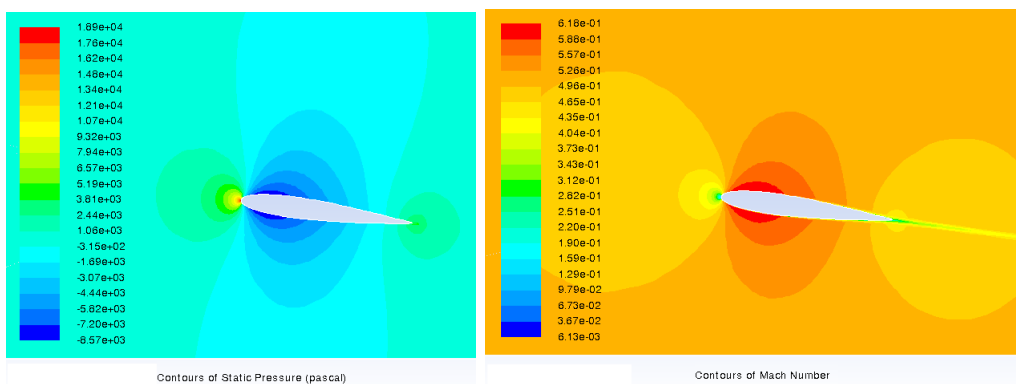


Figure 19: Static pressure and Mach number with Spalart-Allmaras turbulence model.

We notice that the pressure is uniform on the upper and lower side of the wing which is coherent with the angle of attack : there is no lift and almost no drag (a very thin one visible

on the Mach number representation). Moreover, we find a strong static pressure in the front of the wing with is also consistent with a zero angle of attack. **For $\alpha = 4$ we have :**

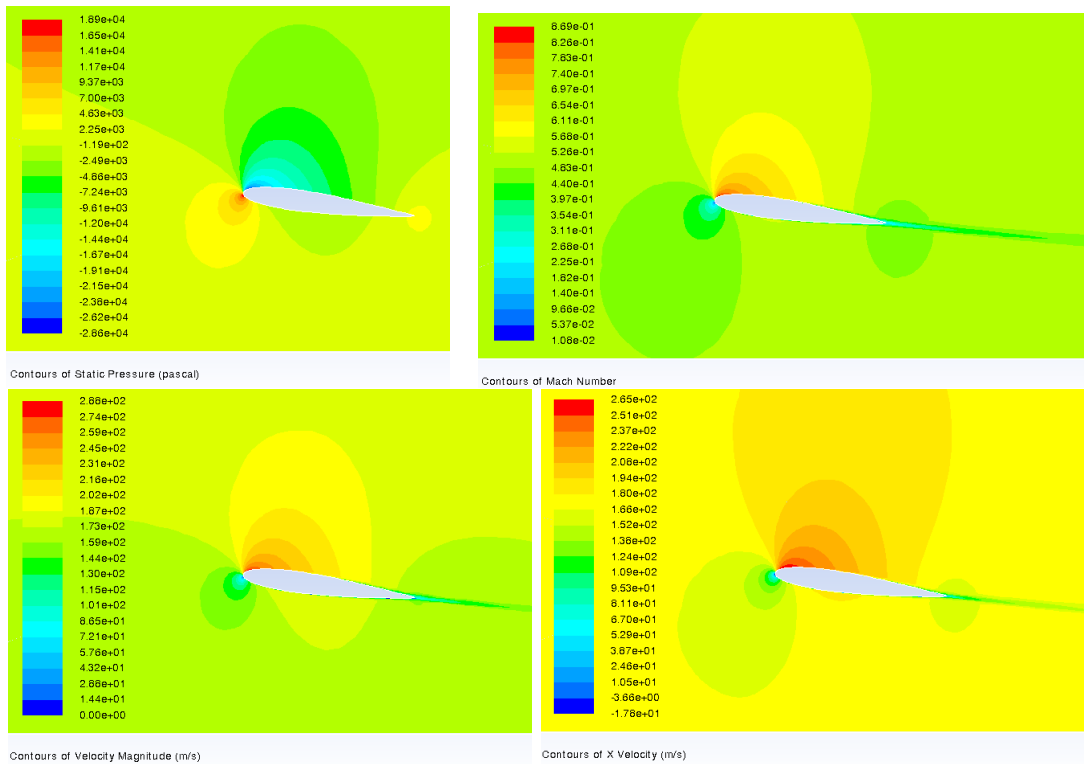


Figure 20: Static pressure, Mach number, velocity magnitude and x-velocity.

The suction and pressure side are clearly visible on the contours of static pressure graph and we notice the good behaviour of the velocity with respect to the pressure variations. Concerning the Mach number, it is increasing in the suction side and we start to observe a more important drag than before. The results for $\alpha = 8^\circ$ were still consistent with the physics, but not relevant to present here. It is more interesting to see the effects on the drag with a large angle of attack that is why we will now present the results for $\alpha = 14$:

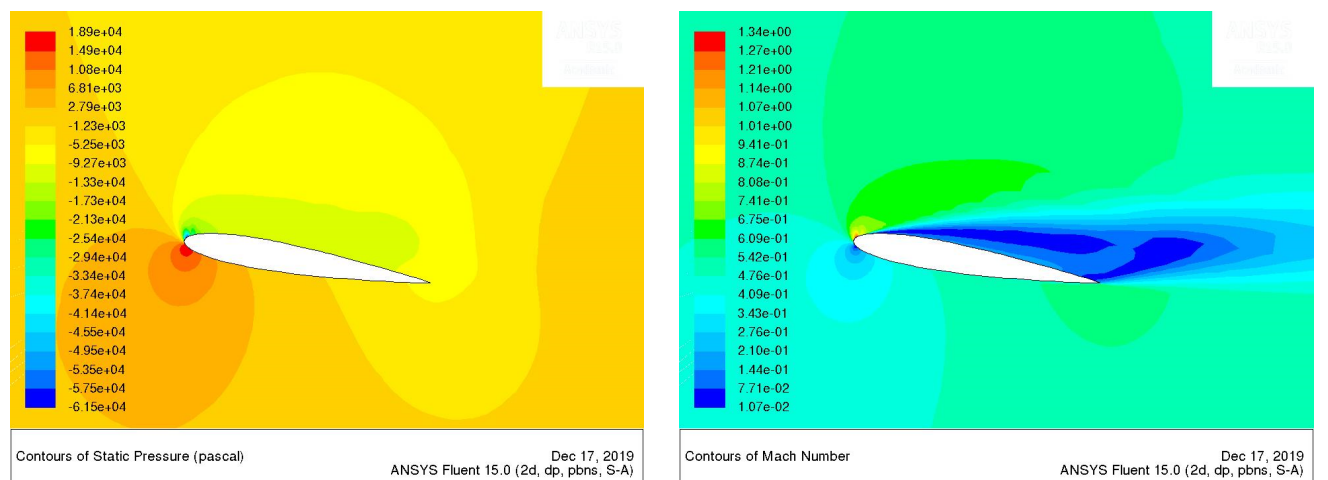


Figure 21: Static pressure and Mach number contours.

We notice a huge drag on the figure on the right represented in blue by a low Mach number area (which is linked with a low velocity area for the air field).

Here we have another data that we had in the class and which closed to the above data, but now for $M_\alpha = 0.5$ and $M_\alpha = 0.7$ with C_L and C_d in different models (Spalart-Allmaras and k-epsilon turbulence models). The k-epsilon model is denoted by the index 2 on the drag and lift coefficients.

	0.5	0.5	0.7	0.7		
0	-8.65E-09	0.007759	3.35E-05	0.01518	0.00	8.90E-03
2	0.25656	8.21E-03	0.6467	0.017618	0.26	9.22E-03
4	0.51207	9.62E-03	1.1977	0.0489	5.09E-01	1.07E-02
6	0.76454	0.012111	1.2113	0.10018	7.61E-01	1.34E-02
8	0.94288	0.02124	1.0919	0.1585	9.43E-01	2.27E-02
10	0.9368	0.04608	1.0963	0.22908	9.78E-01	4.28E-02
12	0.81625	0.10532	1.1529	0.30766	8.81E-01	7.38E-02
14	0.70437	0.14954	1.2358	0.3904	7.89E-01	1.05E-01
	$c_l, m=0,5$	$c_d, m=0,5$	$c_l, m=0,7$	$c_d, m=0,7$	$c_{l2}, m=0,5$	$c_{d2}, m=0,5$

This enable to plot the variation on drag and lift coefficient with respect to the angle of attack and for various Mach numbers, and we obtain the following graphs :

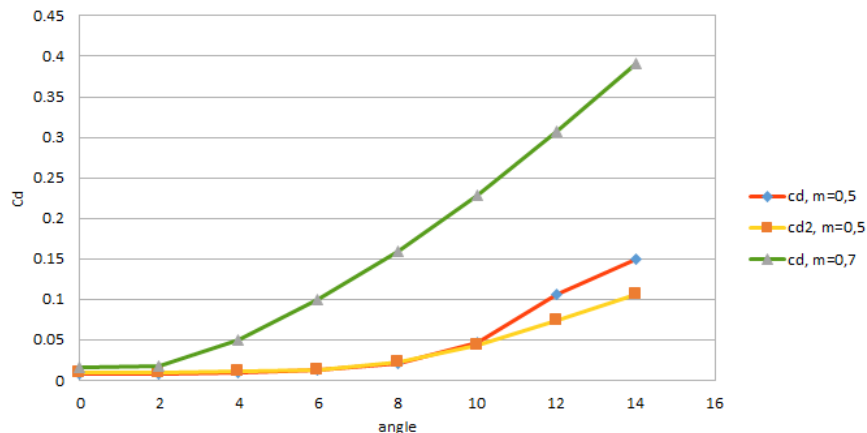


Figure 22: Evolution of the drag coefficient in function of α .

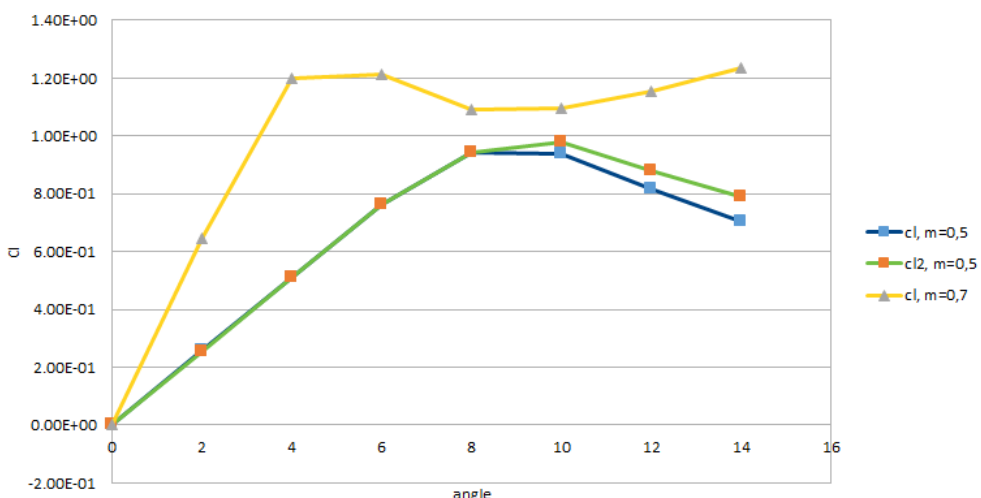


Figure 23: Evolution of the lift coefficient in function of α .

The two turbulent models give a close approximation of the drag and lift coefficients. We notice that in the drag's graph the changes happened after $\alpha = 10^\circ$ so the changes occurs after high α . Similarly, for the lift's graph but the changes happened after $\alpha = 8^\circ$. It means that the results become different when the physics becomes more complex that is why we have to be aware of the modelling choices. We can also observe that for a higher Mach number $M_\alpha = 0.7$, there is a translation in the coefficients which take higher values. Finally, the curves are consistent with the reference ones given by **1973 Gregory Wilby High Mach Number**.

3 elsA - ONERA software for compressible flows.

First, let us present some generalities and main features of the elsA software. The elsA multi-application CFD simulation platform deals with internal and external flows which relies on the solving of the compressible 3D Navier-Stokes equations. It means that this software enables the simulation of compressible flows. A large variety of turbulence models as well as numerical flux models are implemented in elsA.

The system of equations is solved by a cell centered finite-volume method. Space discretization schemes include classical second order centered or upwind schemes and higher order schemes. The mostly used integration of the semi-discrete equations relies on a backward Euler technique with implicit schemes solved by robust LU relaxation methods. However, we will not use convergence criterion (as residuals criterion for instance) but only a number of iterations to end the simulation. The user interface of the software is done in Python.

For each simulation, we will have to define the computational domain by identifying the boundary indexes on the given mesh. To do that, we used Paraview to recover the mesh points located on the boundaries and make the link between the elsA simulation and the results visualization on Paraview. We also have to define the global parameters including the space and time discretization methods, the resolution solver, the types of boundary conditions and initial conditions for time-dependent systems. At the end of the simulation, elsA softawe provides results on the conservative variables which are ρ , $\rho\vec{v}$ and ρE coming form the conservative expressions of the main conservation laws (mass, momentum and Energy). It means that if we need results on the other variables we will use the Paraview calculator and enter the corresponding expressions by hand.

We will present here three test cases : the Naca and Nozzle simulations which we will compare with the Fluent results and a shock tube test case.

3.1 Naca test case

3.1.1 Problem Description

We will consider the simulation of a flow around a Naca0012, which consists in the same simplified structure as presented in Figure 18. The simulation covers a 2D approximation of an aircraft wing and we study the air flow around the wing with an angle of attack of 4° at Mach 0.5.

3.1.2 Equations

Air is considered as a **perfect gas** (it will provide the equation of state), and we will use the **laminar Navier-Stokes**² equations for the simulations. The choice of laminar model is an assumption, and it will enable us to make a comparison with the turbulent model used in Fluent. The model chosen is **steady**, the fluid is **compressible** regarding to the Mach number. Thus the physical equations governing the simulation are :

$$\left\{ \begin{array}{l} \vec{\nabla} \cdot (\rho \vec{v}) = 0 \\ \vec{\nabla} \cdot (\rho \vec{v} \vec{v}) = -\vec{\nabla} P + \vec{\nabla} \tau \\ \vec{\nabla} (\rho E \vec{v} + P \vec{v} - \tau \vec{v} + \vec{q}) = 0 \\ P = \rho R T \end{array} \right.$$

²We neglect gravity effects to study the air flow around the wing.

We impose no slip condition on the wings by taking the **walladia** option (it means adiabatic wall with no thermal changes and no slip condition) which enable to take into account friction phenomena. The initial field is given by a far-field state called **StateInf** : it provides the boundary conditions for boundaries far from the wing. This far-field state is given by the following parameters with the usual notations : $M_{inf} = 0.5$, $T_{inf} = 293.15\text{K}$, $\rho_{inf} = 1.2 \text{ kg.m}^{-3}$ and then we compute $\rho E := RoeInf$ and each component of $\rho \vec{v}$ denoted by $RouInf$, $RovInf$ and $RowInf$ for the x,y and z direction respectively. We have :

$$\begin{aligned} RouInf &= \rho_{inf} v \cos(\alpha) \\ RovInf &= \rho_{inf} v \sin(\alpha) \\ RowInf &= 0 \\ RoeInf &= 0.5\rho_{inf}v^2 + T_{inf}C_v \end{aligned}$$

with $v = M_{inf}\sqrt{\gamma RT_{inf}}$ and α the angle of attack express in radian.

Finally, to compute the numerical flux from a finite volume point of view we use the Roe and Jameson flux.

3.1.3 Numerical results

For $\alpha = 4^\circ$ and the Roe flux, we compute the velocity field, the pressure and the mach number using the Paraview calculator and we get the following results for these three parameters :

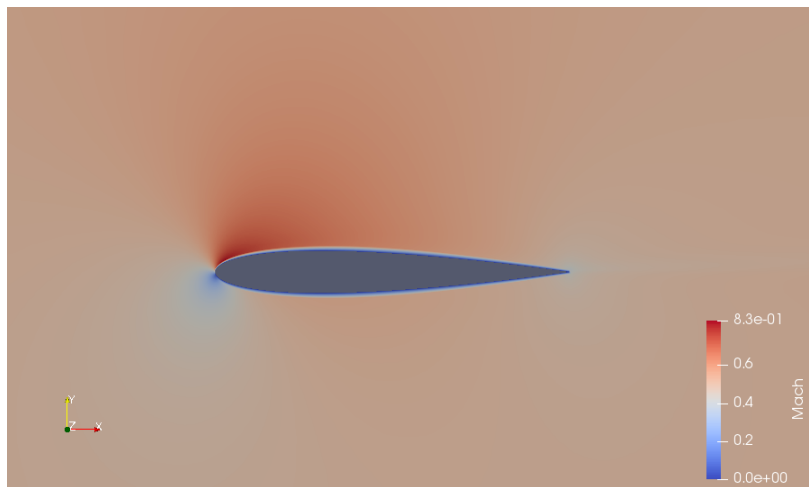


Figure 24: Mach number contours.

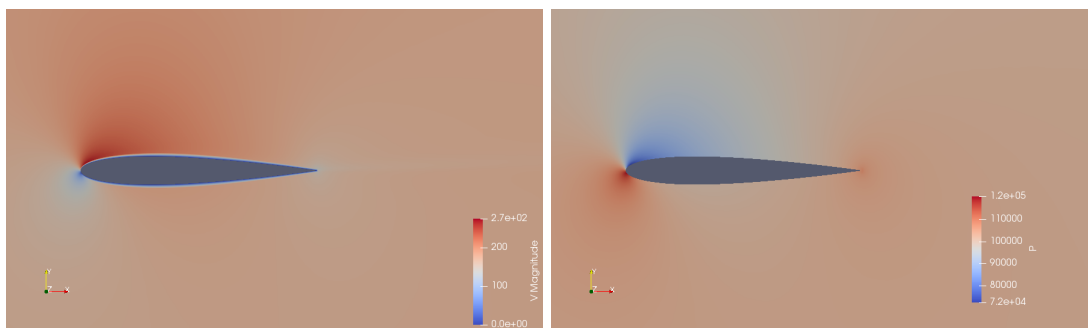


Figure 25: Velocity and pressure contours (respectively on the left and right).

Concerning the pressure contours, we observe a drop of pressure on the upper side of the wing which corresponds to the suction side, and an increase in pressure on the bottom or pressure side : this variation in pressure generates the lift (a strength from high to low pressure). The behaviour of the velocity is the reverse which is consistent and we notice a little drag effect on light blue at the back of the wing. Besides, the no slip condition is clearly visible on the velocity contours since we have $v = 0$ on the wing boundary (the boundary layer is also visible in light blue). The Mach number is about 0.83 on the suction side so it has increased in the same way as the velocity and decreased on the pressure side. In the Fluent simulation, with turbulent model, the Mach number was about 0.86 at its higher value. In a general way, we obtain downward values for the velocity and Mach parameters in elsA simulation compared to Fluent. However, the Jameson flux approximation provides results which are closed to the Fluent simulation even with a different physical model (laminar instead of turbulent) as it is shown in the following figures :

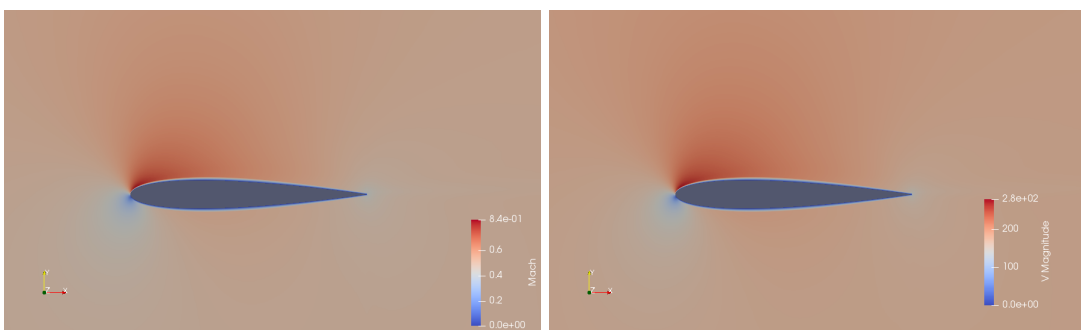


Figure 26: Mach number and velocity contours.

3.2 Shock tube test case

3.2.1 Problem Description

In this part, we have considered the example of a Shock tube which is a device to study shock wave. It means that there is fluid (typically air) in a medium separated by a wall which block any flow, the pressure is increased in a part of the medium to create a huge variation. Then the wall is removed at time $t = 0$ and the gas expands down the other half of the tube generating a shock wave.

3.2.2 Equations

For this simulation, air is taken as **perfect gas** and **compressible**, we will neglect both gravity and friction effects. It means that we will use the **Euler Equation** instead of the usual Navier-Stokes. The system will be time-dependent so **unsteady** and we will use two different numerical fluxes (Roe flux and AUSM flux). The initial conditions for each part of the medium are given in the following table :

$x < 0$	$x \geq 0$
$\rho_G = 1.18 \text{ kg.m}^{-3}$	$\rho_D = 0.15 \text{ kg.m}^{-3}$
$P_G = 101325 \text{ Pa}$	$P_D = 10132.5 \text{ Pa}$
$E_G = 2.5 \text{ J.kg}^{-1}$	$E_D = 2 \text{ J.kg}^{-1}$
$V = 0 \text{ m.s}^{-1}$	

Finally, we have the following system of equations given by the conservation laws :

$$\begin{cases} \frac{\partial \rho}{\partial t} + \vec{\nabla} \cdot (\rho \vec{v}) = 0 \\ \frac{\partial(\rho \vec{v})}{\partial t} + \vec{\nabla} \cdot (\rho \vec{v} \vec{v}) = -\vec{\nabla} P \\ \frac{\partial \rho E}{\partial t} + \vec{\nabla} \cdot (\rho E \vec{v} + P \vec{v} + \vec{q}) = 0 \\ P = \rho R T \end{cases}$$

3.2.3 Numerical results

We have used both Roe and AUSM flux and they give similar results, so we only present the pressure and Mach number contours for one of them.

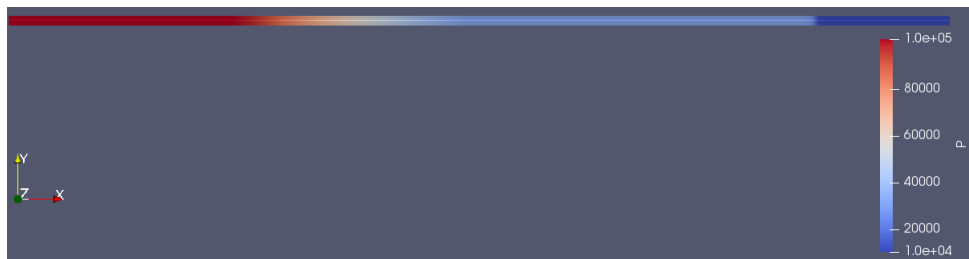


Figure 27: Pressure at time $t = 7 \times 10^{-3}$ s with Roe flux.

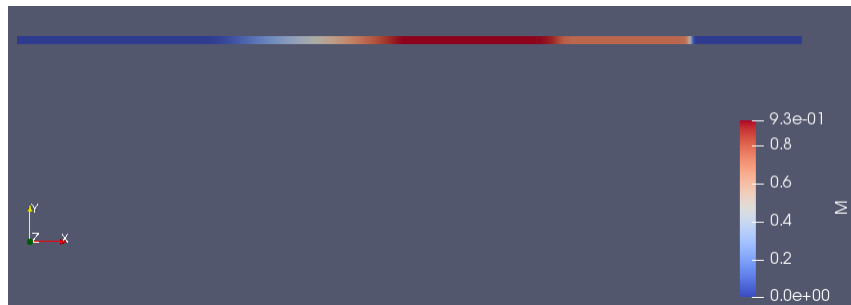


Figure 28: Mach number at time $t = 7 \times 10^{-3}$ s with Roe flux.

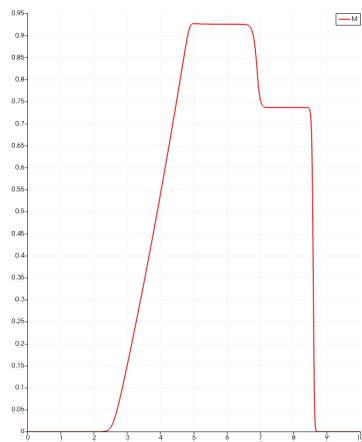


Figure 29: Spatial Mach evolution : fast and high variations.

The fluid is going from the high pressure to the low pressure area and the drop in static pressure generates an sudden increase in Mach number and thus the shock wave. The evolution of the Mach across the shock wave is given by the curve on Figure 29. As we have an analytical solution, we can compare it with the numerical results for Roe and AUSM flux : this is done for the density and pressure and given by the following figures :

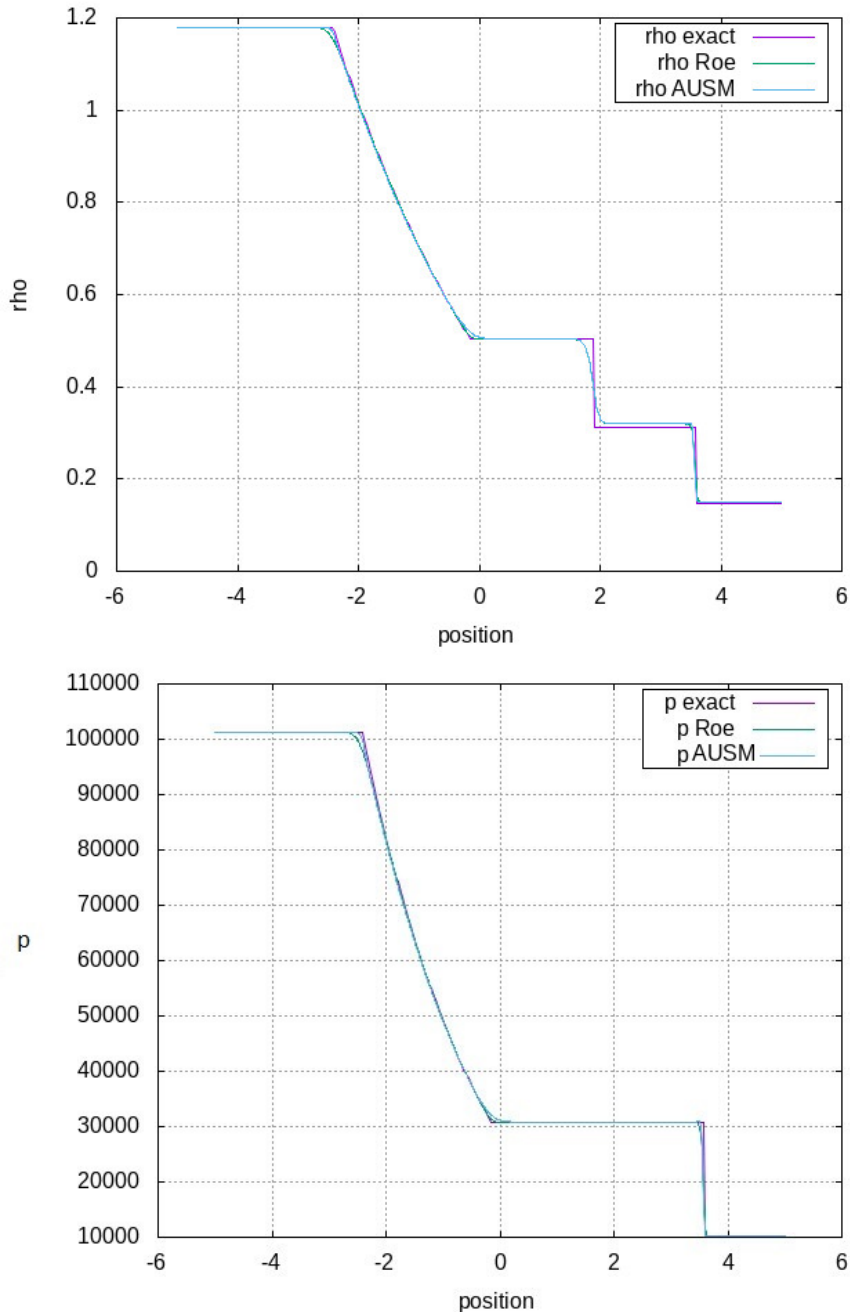


Figure 30: Comparison between numerical and exact solutions for pressure (bottom) and density (top) parameters.

The exact solution shows the shock waves with very stiff angle when sudden changes in parameters occur but numerically, smooth curves are used to approximate the shock. To capture the shock, we must find the best numerical scheme : regarding to the curves, it seems that the AUSM flux gives a better approximation.

3.3 Nozzle test case

3.3.1 Problem Description

In the sequel, we consider the simulation of a subsonic **steady state** internal flow in a nozzle. The geometry of nozzle is known and analytical solutions are well-known in the subsonic regime so we can compare results (a section on the central axis) to the analytical solution (pressure and Mach number) for an inlet Mach number of 0.036.

3.3.2 Equations

We consider the **Euler equation** neglected gravity with **perfect gas** equation of state. Regarding to the Mach number we are in an **incompressible** case : we are in fact, in a particular case that enables to take very low Mach number even if elsA is done for compressible flow computation. It means that we consider the following equations :

$$\begin{cases} \vec{\nabla} \cdot (\rho \vec{v}) = 0 \\ \vec{\nabla} \cdot (\rho \vec{v} \vec{v}) = -\vec{\nabla} P \\ \vec{\nabla} (\rho E \vec{v} + P \vec{v} + \vec{q}) = 0 \\ P = \rho R T \end{cases}$$

We define an initial state for which the conservative variables are given, especially we have $P_{in} = 101300$. We impose the outlet pressure equal to the initial one and then we compute the inlet pressure using the following relation :

$$P_{inlet} = P_{outlet} \left(1 + \frac{\gamma - 1}{2} M^2 \right)^{\frac{\gamma}{\gamma - 1}}.$$

3.3.3 Numerical results

The geometry of the mesh is not really precise if we compare with the Fluent simulation : the throat of the nozzle is more or less approximate by a straight line.

Concerning the Mach number evolution, we have done a plot over line along the central axis and we recover the same shape for the curve on Figure 32 and Figure 17. It means that the Mach number is increasing in the throat region at the same time that the pressure decreases.



Figure 31: Pressure contours.

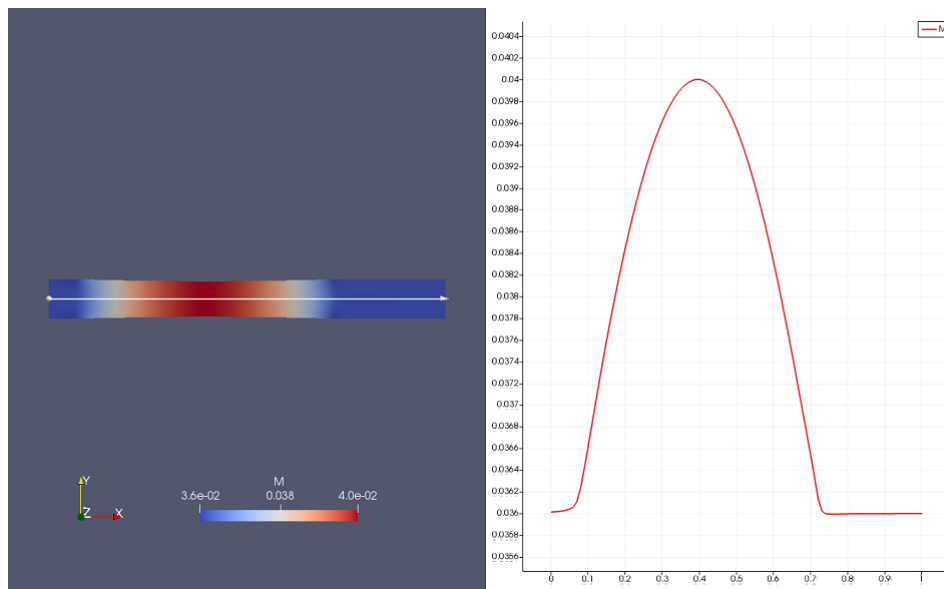


Figure 32: Mach number contours and evolution along the central axis.

We have then compared these numerical results with the analytical solution, and we obtain the following curves :

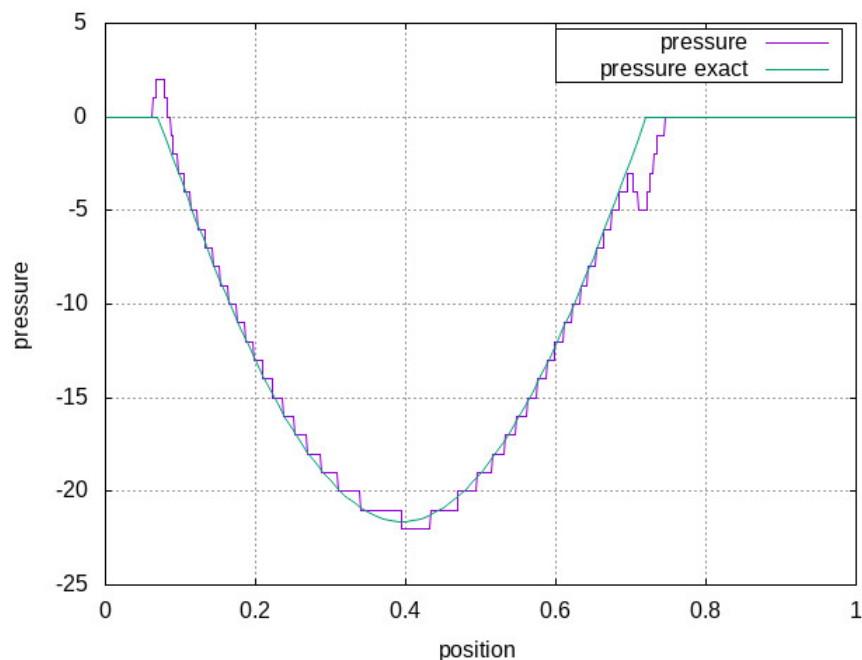


Figure 33: Comparison numeric and analytical solutions for pressure.

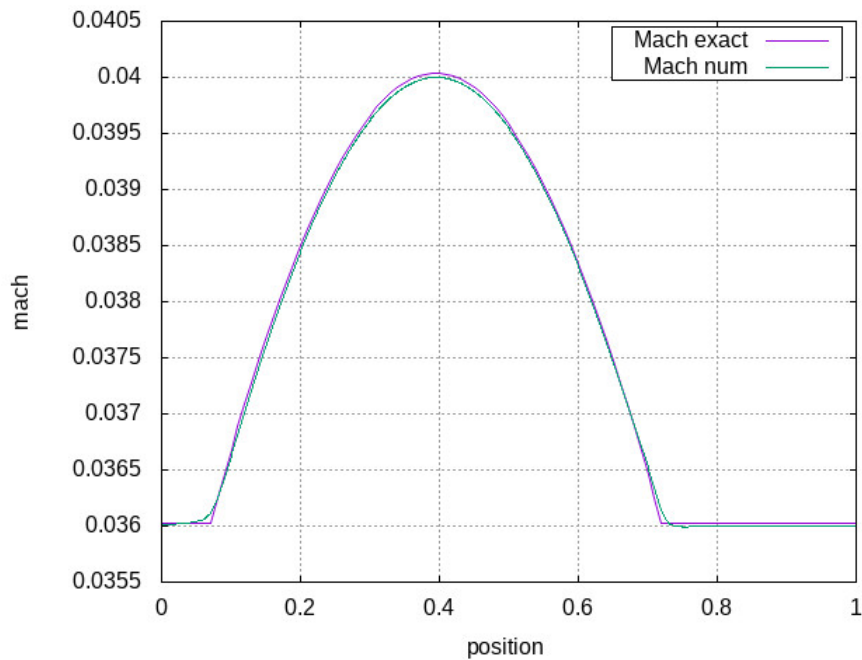


Figure 34: Comparison numeric and analytical solutions for Mach.

The numerical scheme creates some fluctuations on the pressure curve, but the global shape corresponds to the exact solution and for the Mach number, we have a good approximation by a smooth curve.